Journal of Hydrology 567 (2018) 489–509

Contents lists available at ScienceDirect

Journal of Hydrology

journal homepage: www.elsevier.com/locate/jhydrol

Research papers

Investigation of multi-model spatiotemporal mesoscale drought projections over India under climate change scenario

Vivek Gupta*, Manoj Kumar Jain

Department of Hydrology, Indian Institute of Technology Roorkee, Uttarakhand, India

ARTICLE INFO

This manuscript was handled by Andras Bardossy, Editor-in-Chief, with the assistance of Saman Razavi, Associate Editor

Keywords:
Droughts
Climate change
K-means clustering
Spatiotemporal analysis
Fourier periodicity analysis

ABSTRACT

Projected droughts for 21st century over India have been analysed using precipitation and temperature data obtained from Regional Climate Models (RCMs) under Representative Concentration Pathways (RCPs) 4.5 and 8.5. Standardized Precipitation Index (SPI), Standardized effective Precipitation Evapo-Transpiration Index (SP*ETI) and Standardized Precipitation-Evapotranspiration Index (SPEI) at the timescale of 12-months have been used for drought characterization. The K-means clustering algorithm has been utilized to delineate distinct drought homogeneous regions in India. Trends and periodicities in drought characteristics have also been analysed. The results of this study reveal that increase in evapotranspiration due to projected rise in temperature would play a major role in affecting future drought dynamics in most parts of India. Analysis indicates that computed magnitude of drought intensity, duration and frequency depends on the choice of drought indicator. SPEI drought index has been found to project highest drought risk as compared to other two indices used in this study. North India is more vulnerable to increase in drought severity and frequency in near future. However in far future, most parts of the country, except few southeastern states, are likely to face an escalation in drought severity and frequency. A shift in drought hazard from central India toward southeast-central India is likely to happen with increase in greenhouse gas (GHG) concentration. The areal extent of droughts has been found to be increasing historically which is expected to increase further in future for most parts of the country. Historically, drought dynamics were more influenced by decrease in precipitation. However, in future, the drought dynamics will be significantly influenced by increased evapotranspiration resulting from increase in temperature in spite of likely increase in precipitation. The periodicity analysis indicates inter-annual periodicities influencing monsoon months to be distributed uniformly across all clusters of the Indian subcontinent with dominant cycles of 2–3.6 years. Further, change in periodic cycles of drought due to climate change is found to be insignificant.

1. Introduction

Drought is one of the costliest and widespread long term persistent natural phenomena, that may last for weeks, months, years or even decades (Xu et al., 2015). More than one million lives have been lost globally since 1974 due to droughts (UN, 2008). Therefore, systematic information about likely occurrence and distribution of droughts may assist in preparedness and mitigation against drought disasters (Lloyd-Hughes, 2012). The preparedness and planning to cope with adverse impacts of a drought event depend on the information about its areal extent, severity and duration. This information could be obtained through drought monitoring using various drought indices that provide quantitative information to the decision makers about drought characteristics (Dogan et al., 2012). A variety of meteorological drought indicators such as Palmer Drought Severity Index (PDSI; Palmer, 1965), Rainfall Decile based Drought Index (RDDI; Gibbs and Maher, 1967), Bhalme and Mooly Drought Index (BMDI; Bhalme and Mooley, 1980), Standard Precipitation Index (SPI; McKee et al., 1993), Effective Drought Index (EDI; Byun and Wilhite, 1999) etc. have been developed to monitor and quantify meteorological droughts. The choice of drought index depends on the perspective and the scope of the problem at hand.

India is one of the most drought-affected countries in the world (Mishra and Singh, 2011) and faces drought in almost every three years in different parts of the country (Goyal et al., 2017). About 94 million-hectares area of the country is drought prone with more than 300 million people being impacted (Gupta et al., 2011). In previous few decades, India experienced prolonged and widespread droughts in different parts of the country, and the frequency of droughts has also increased in the recent times (May 2002). The drought of 2002 alone

* Corresponding author.
E-mail address: vgupta@hy.iitr.ac.in (V. Gupta).

https://doi.org/10.1016/j.jhydrol.2018.10.012
Received 14 April 2018; Received in revised form 4 September 2018; Accepted 6 October 2018
Available online 09 October 2018

resulted in the reduction of the net sown area by 12 million hectares and the consequent reduction in food grain production by 38 million tons, which resulted in a 3.2 percent decline in agricultural GDP (Rathore et al., 2014). A major amount of annual rainfall (about 70–90%) in India occur due to southwest monsoon during the months of June to September. A large deficit in monsoon rainfall may lead to drought conditions over India (Kumar et al., 2013). Numerous studies can be found in the literature that bring out the analyses of occurrence and distribution of different types of droughts that had occurred in the past in India (Das et al., 2016; Jain et al., 2015; Janga Reddy and Ganguli, 2012, Naresh Kumar et al., 2012; Guhathakurta and Rajeevan, 2008; Chowdhury et al., 1989). Droughts in India are becoming more regional and a spatial shift toward coastal south India, Central Maharashtra and Indo-Gangetic plains have been observed (Mallya et al., 2016). Number of wet days during monsoon along the east coast have decreased significantly during monsoon, pointing to more intense rainfall events and prolonged dry spells (Sen Roy and Balling, 2004). Upper and middle Gangetic plains, central and eastern plateau and central and eastern hills have witnessed significantly drying trends during the whole duration of summer in the previous decades (Jha et al., 2013). However, global warming and subsequent climate change may further affect the drought vulnerability profile of a country (O'Brien et al., 2004). Increase in temperature of the order of 0.57 °C per 100 years has been observed in India (Kumar et al., 1994; Lal and Singh, 2001). Therefore, knowledge of probable drought scenarios in the near future could be of immense use for decision makers and planners to formulate appropriate policy framework to minimize the impacts of drought hazard on the overall development of the country.

Climate projections are being used widely for assessing drought conditions for the 21st century on global as well as regional scales (Strzepek et al., 2010; Orlowsky and Seneviratne, 2013; Dai, 2013; Xu et al., 2015; Wang and Chen, 2014; Masud et al., 2017; Thilakarathne and Sridhar, 2017). However, the uncertainty associated with climate projections should be kept in view during the examination of future drought scenarios. Sheffield et al. (2012) concluded that the changes in drought climatology in recent years are insignificant. However, Dai (2013) found that droughts are intensifying due to global warming. These contrasting results may be attributed to the limitations of the current climate models in capturing the regional rainfall (Turner and Annamalai, 2012). Lin et al. (2015) found drying tendency in southwestern China in the 21st century, which may intensify due to augmented carbon emissions. Cook et al. (1999) argued that the drought risk in the 21st century is going to exceed the driest century of Medieval Climate Anomaly for both moderate and high emission scenarios in Southwest and Western North America. Swain and Hayhoe (2015) reported that northern regions of North America show consistent trends of wetting and at the same time, the south-western parts of continent show trends of drying which may further intensify due to increased warming. In the Indian context, very few studies have been reported on the analysis of drought scenarios incorporating climate projections. But, many studies have been conducted on the spatiotemporal distribution of Indian monsoon rainfall with contrasting outcomes. Some studies have established an increase in the average monsoon precipitation along with an inter-annual variability of precipitation (Chaturvedi et al., 2012; Fan et al., 2012; May 2002; Cubasch et al., 2001; Lal et al., 2001). However, other studies have established a suppression in monsoon rainfall in future due to weakening of monsoon circulation and reduction in intra-seasonal modes (Ashfaq et al., 2009; Tanaka et al., 2005; Ueda et al., 2006).

The present study is aimed at an investigation of the spatial and temporal projections of droughts for different climate change scenarios over India. Changes in the trends and periodicities of the severity and frequency of drought over India with climate change is investigated. Influence of increasing evapotranspiration because of rising trend in temperature due to climate change, on the drought dynamics has also been investigated. Finally, the spatial distribution of drought hazard for 21st century is examined.

2. Data and methodology

2.1. Selection of RCMs for the future projected precipitation data

Regional Climate Models (RCM) are the physics based higher spatial resolution models which are derived from the GCM models by dynamic downscaling of the GCM data. However, the selection of GCMs impose great uncertainty on the final climatic projection for a particular region (Knutti and Sedláček, 2013). Chaturvedi et al. (2012) found that the GFDL-CM3 model is the best among individual models for simulating historical precipitation, followed closely by the several other models, such as GFDL ESM2G, GFDL ESM2M, HadGEM2-ES, HadGEM2-AO, etc. For the Asian summer monsoon, Sperber et al. (2013) developed skill metric for 25 CMIP5 and 23 CMIP3 GCM models and found that top five skill scorers for precipitation are CNRM-CM5, NCAR-CCSM4, NorESM1-M, GFDL-CM3 and GFDL-cm2.1. Sengupta and Rajeevan (2013) analyzed the performance of various GCMs using reliability ensemble averaging technique (REA) and found GFDL-CM3, MPI-ESM-LR, NorESM 1-M, LASG-FGOALS-G2, CNRM-CM5 among the top five performing model with least bias for precipitation. McSweeney et al. (2015) categorized HadGEM2-ES, CCSM4, CNRM-CM5, MPI-ESM-LR, MPI-ESM-MR, GFDL-ESM2G, GFDL-ESM2M and GFDL-CM3 models as 'satisfactory', for the South Asian region, for simulating the northeast monsoon, annual cycles of temperature and precipitation, summer monsoon and summer monsoon indices. Based on the suitability of different GCMs, corresponding RCM models have been selected for this study for further analysis as shown in Table 1. Outputs of most of the RCMs are generally available at 50 km spatial resolution, however, the observed data is available at 0.5-degree spatial grid. Therefore, it is necessary to bring all the datasets under the same resolution (spatial and temporal) for analyzing the historical and future projected precipitation. Therefore, all the model outputs have been converted to the reference 0.5° grid using bilinear interpolation. Observed precipitation data originally available for 0.25° grid (Pai et al., 2014) have also been aggregated to 0.5° reference grid resolution.

2.2. Drought indices, drought events and their characteristics

Drought indices (DI) are the numeric indicators which assimilate one or more climatic variables such as precipitation and

Table 1
Details of regional climate models used in this study.

Sr. no.	Institute	Driving Model	RCM Model	Period	Spatial resolution	RCP available
RCM1	Canadian Centre for Climate Modelling and Analysis (Canada)	CCCma-CanESM2	IITM-RegCM4	2006–2099	50 km	RCP4.5, RCP8.5
RCM2	Centre National de Recherches Météorologiques (France)	CERFACS-CNRM-CM5	IITM-RegCM4	2006–2085	50 km	RCP4.5, RCP8.5
RCM3	NOAA Geophysical Fluid Dynamics Laboratory (USA)	GFDL-ESM2M	IITM-RegCM4	2006–2099	50 km	RCP4.5, RCP8.5
RCM4	Hadley Center for Climate Prediction and Research (UK)	HadGEM2	SMHI-RCA4	2006–2099	50 km	RCP2.6,RCP4.5, RCP8.5
RCM5	Max Planck Institute for Meteorology(Germany)	MIROC5	SMHI-RCA4	2006–2100	50 km	RCP2.6, RCP4.5, RCP8.5
RCM6	Max Planck Institute for Meteorology(Germany)	ESM-LR	CSC-REMO2009	2006–2100	50 km	RCP2.6, RCP4.5, RCP8.5
RCM7	Max Planck Institute for Meteorology(Germany)	ESM-MR	IITM-RegCM4	2006–2099	50 km	RCP4.5, RCP8.5

evapotranspiration into a single numerical value to quantify the drought characteristics. Various drought indices are available in the literature to quantify droughts. However, the selection of drought indices depends on their suitability to the local climatic scenario and the goals of a particular study. For analysing meteorological droughts, Palmer Drought Severity Index (PDSI), Standardized Precipitation Index (SPI, McKee et al., 1993) and Standardized Precipitation-Evapotranspiration Index (SPEI, Vicente-Serrano et al., 2010) are the most commonly used indices (Mishra and Singh, 2011). PDSI was mainly developed for the United States thus it is mainly used in the United States. It has little applicability outside the United States (Kogan, 1995) because PDSI does not perform well in the regions where the variability in rainfall extremes is more (Burke et al., 2006; Wang et al., 2017). SPI gained popularity because it is simple to compute and require less data. The SPI can be estimated at different time scales and, therefore, it provides flexibility to account for the impact of rainfall deficit of different durations on different water resource components (McKee et al., 1993). However, SPI does not take evapotranspiration (ET) into account and, therefore, it does not consider the true availability of water. SPEI takes advantage of both the PDSI and SPI indices. It takes advantage of PDSI's sensitivity to the evaporation demand due to temperature fluctuation as well as of that of SPI's multi-temporal nature in its estimation. However, SPEI has been found to show stronger drying as compared to its hydrologic benchmark since it takes ET at the potential rate which is less practical (Joetzjer et al., 2013). Considering actual evapotranspiration in the estimation of SPEI shows consistency in drought index with Standardized Runoff Index (Joetzjer et al., 2013). Therefore, Maccioni et al. (2014) developed a new Standardized Effective Precipitation EvapoTranspiration Index (SP*ETI), which not only considers ET but also effective precipitation i.e. precipitation available for ET and losses of water due to runoff and, thereby, representing the realistic ET scenario (Maccioni et al., 2014). In this study, three drought indices namely, the SPI, SP*ETI and SPEI have been used to investigate the spatio-temporal characteristics of droughts in India for the 21st century. All these indicators can be assessed on a time scale ranging from 1 month to as long as 48 months thus representing the short-term water deficit to multi-year storage deficit causing the overall meteorological, hydrological and agricultural drought (Jain et al., 2015; Livada and Assimakopoulos, 2007; McKee et al., 1993; Maccioni et al., 2014). Longer time scales such as 12 or 24 months identify dry periods of relatively longer durations for analyzing the hydrological impacts of drought on streamflow, reservoir levels and groundwater levels (Vicente-Serrano, 2006). Procedure for estimating the SPI, SP*ETI and SPEI are similar. The first step is to calculate reference variable X. For SPI, the reference variable is the average monthly precipitation; however, for SPEI the reference variable is estimated using the following equation;

$$X(i) = P(i) - PET(i) \quad (1)$$

where P is the monthly precipitation and PET is the monthly evapotranspiration for the *ith* month. Vicente-Serrano (2006) suggested the estimation of PET using Thornthwaite method (Thornthwaite, 1948) due to its simplicity and requirement of only average monthly temperature as input. However, for SP*ETI, reference variable can be estimated using following equation.

$$X(i) = P(i) - EP(i) \quad (2)$$

where EP is the effective precipitation which can be estimated using the Soil Conservation Service (SCS) formula (USDA, 1970) which is used widely in agricultural water management practices. Reference variable is cumulatively added for a time window of *t*-months and a resulting series X_t is prepared. For the Indian condition, where most of the rainfall is received during the monsoon lasting for four months followed by a nearly dry period of eight months, hydrologic regimes in the context of drought analysis would be better assessed using 12-month time scale. Many studies have also used the 12-month time scale for examining the drought characteristics in India (Praveen et al., 2016; Saha et al., 2015; Shah et al., 2015). Therefore, a 12-month running time series X_{12} is used to evaluate the SPI, SP*ETI and SPEI indices.

Next step of drought computation involves identifying the best fit distribution for the reference variable and estimation of parameters of the distribution. Method of moments (MOM), is the most widely used method for the estimation of parameter of a probability distribution. But, parameters obtained using the MOM have been found to be less accurate than other methods such as maximum likelihood estimation (MLE), method of probability weighted moments (PWM) and Method of L-moments (MLO). MLE is also very widely used method due to its invariance properties of sufficiency, consistency, efficiency and parameterization invariance properties (Myung, 2003) but MLE can be trapped with local minima if provided with the wrong initial guess of parameters. The parameters estimated using the L-moments method provides a robust estimation and are less sensitive to outliers. Therefore, method of L-moments is used in this study to identify the best-fit distribution with the help of Bayesian Information Criteria (BIC). The identified drought indices for this study are computed for individual grid cells and later used to obtain the regional characteristics using the regionalization analysis. Distributions with two parameters such as Gamma, Gumbel, Logistic and Normal distributions can be used for the computation of SPI since cumulative values of precipitation do not contain negative values and choosing an extra location parameter may truncate the distribution at zero. However, for the estimation of SPEI and SP*ETI indices, distributions with location parameter such as the Generalized extreme value, Generalized logistic, Normal and Pearson type 3 distribution have been used since the climatic water balance is not bounded by zero and may take negative values therefore a location parameter is required. Python 'lmoments3' library has been employed to identify the best distribution. For finding the cumulative probability for selected distribution, the parameters obtained from L-moments are used to initialize the maximum likelihood optimization using 'SCI' package in R. Further, the estimated probabilities have been converted to normally distributed series with zero mean and unit variance using inverse Gaussian function (Farahmand and AghaKouchak, 2015). For defining various drought characteristics, the theory of run (Yevjevich, 1967) is used considering the time series of all drought indices. Runs approach identifies drought severity, duration, frequency and interval above the chosen values of thresholds. A sequence of consecutive drought indices values below -0.5 is considered as a run. Each run is denoted as an individual drought event as shown in Fig. 1. Length of the run, which is a measure of drought duration, is the time between the beginning and the onset of a drought event. Severity of a drought event is defined based on the cumulative value of SPI, SP*ETI or SPEI series estimated for the drought event.

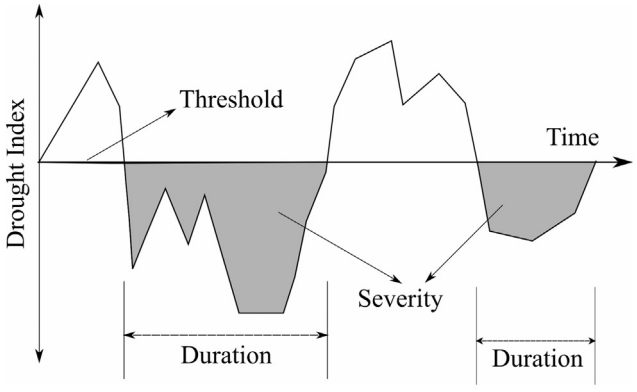

Fig. 1. Application of theory of run.

2.3. Regionalization of droughts

Generally, regionalization methods are used in hydrology for drought and flood frequency analysis. Drought is a regional phenomenon and, therefore, it is appropriate to study the droughts in a regional perspective. Cluster analysis is a broader term applicable for a range of statistical approaches used to estimate the similarity between various individual objects in a group based on certain characteristics. Many methods are available for delineating homogeneous regions such as Region of Influence method (Burn, 1990), entropy-based method (Ridolfi et al., 2016), hierarchical clustering, fuzzy clustering and K-means clustering (Rao and Srinivas, 2006a,b). Machine learning algorithms are easy to implement and provide homogeneous results as compared to other traditional methods (Rao and Srinivas, 2006a; Goyal and Gupta, 2014). Therefore, in this study, K-means clustering algorithm is used for identifying the homogeneous drought regions in India. K-means is a divisive unsupervised learning algorithm developed by MacQueen (1967) for classifying the multivariate data. Eq. (3) shows the objective function which K-means algorithm attempts to minimize.

$$J = \sum_{j=1}^{K} \sum_{i=1}^{M} \|Y_i - C_j\|^2 \tag{3}$$

where $\|Y_i - C_j\|^2$ is squared Euclidean distance between the i^{th} data point and j^{th} cluster centre in multidimensional space of data attributes. M is the total number of data points and K is the number of clusters. Initially, the co-ordinates of K-cluster centres are guessed randomly, and each point is assigned to the nearest cluster centre. Cluster centres are updated by averaging the coordinates in a particular clusters and reassignment is made to obtain new clusters. This process is repeated until the convergence is reached. Since the final result is very sensitive to the initial used cluster centre, the algorithm is repeated again and again with different initial random cluster centres for obtaining the best results (Dalton et al., 2009). A priori estimate of the optimum number of clusters is worked out before applying the K-means clustering algorithm for getting the well separated compact clusters. Cluster validity indices such as Dunn Index (Dunn, 1974), Average Silhouette Width Index (Rousseeuw, 1987) and Davies and Bouldin Index (Davies and Bouldin, 1979) are generally used to obtain an optimum number of clusters. In this study, we have used Average Silhouette Width Index (ASWI) and Davies and Bouldin Index (DBI) for validation of clusters. Details of these indices can be found in Goyal and Gupta (2014). In this study, the drought severity, duration and interval along with the latitude and longitude of grid centre are used as characteristics vector to segregate homogeneous clusters in India.

2.4. Trend analysis

Trend analysis is a widely used nonparametric method for identifying trends in hydrology and climatology. Maidment (1992) recommended the use of the Mann-Kendall non-parametric test as an excellent tool for the detection of trend in a hydroclimatic time series. Mann-Kendall test is a nonparametric test, which tests a hypothesis that data comes from independent realization and are identically distributed. However, this test is only applicable for the data series which is not serially correlated. But, most of the times, hydro-climatic data series violate this assumption (Razavi and Vogel, 2018). Therefore, Von Storch (1999) suggested the prewhitening of the time-series to tackle this issue. Yue and Wang (2004) suggested an approach based on AR1 model to remove the serial correlation which is used in this study. The Mann-Kendall test while removing serial correlation is commonly known as the modified Mann-Kendall test. The sen's slope is generally used for assessing the magnitude of trend based on the median of incremental slopes. More details on these tests can be found elsewhere (Razavi and Vogel, 2018; Gocic and Trajkovic, 2013; Mondal et al., 2012; Tabari et al., 2011). In this study, the trend analysis is performed on severity and frequency of droughts at various grid points. Trends above 95% confidence interval is considered as significant therein.

2.5. Drought hazard Index (DHI)

Quantification of drought hazard requires knowledge of drought severity, duration, frequency and interval of different drought events (Daneshvar et al., 2013). Maccioni et al. (2014) proposed a comprehensive drought hazard assessment index called the Drought Hazard Index (DHI). Computation of DHI involves meta-analysis of drought characteristics of a region derived based on different drought indices such as SPI-12, SP*ETI-12 or SPEI-12. For the computation of DHI, the following four sub-indicators are estimated (Maccioni et al., 2014).

1. The number of drought events observed in a particular period (FRQ).
2. The number of drought events with duration greater than 24 months (FRQ24).
3. The maximum observed severity across the observed episodes (Smax).
4. The maximum duration in months across the drought episodes (Dmax).

Each sub-indicator is divided into four classes assigned with relative scores from 1 to 4 by defining certain thresholds. Thresholds are generally obtained by dividing all the values of a sub-indicator for all the spatial points in equal parts. Then, Eq. (4) is used to compute the DHI

$$DHI = w_1 * score(Dmax) + w_2 * score(Smax) + w_3 * score(FRQ24) + w_4 * score(FRQ) \tag{4}$$

where w_i are the relevant weights which are estimated using an analytical hierarchical process (AHP; Saaty, 1977; Maccioni et al., 2014). In the present study, the DHI is computed for the SPI-12, SP*ETI-12 and SPEI-12 for inter-comparison purposes.

2.6. Periodicity analysis

Almost all climatic time series possess inherent cycles of different periods. Cyclicity analysis may provide an insight into the hidden periodicities of the climatological data series. Various methods have been used to find cyclicity in hydro-climatic variables (Salamalikis et al., 2016; Pathak et al., 2016; Yuan et al., 2015; Zhang et al., 2014; Wu et al., 2013). Different approaches of Fourier transform (also called spectral analysis) and wavelet transform analysis are the most widely used techniques for periodicity analysis (Moreira et al., 2015; Telesca et al., 2013; Yadava and Ramesh, 2007; Bordi et al., 2004). Fourier analysis is generally utilized for extracting regular cyclical component and finding the periodicities in time series. Fourier analysis comprises of decomposition of a time series as various sinusoidal functions (Bloomfield, 2004; Pollock et al., 1999). Therefore, a cyclic time series is written in the form

$$y_t = \sum_{j=0}^{m} [A_j \sin(\omega_j t) + B_j \sin(\omega_j t)] + \epsilon_t \tag{5}$$

where t is time, A_j and B_j, j = 0,…,m are the parameters and ϵ_t, t = 1, …,n are the identically independent random variables with zero mean and unit variance. Value of $m = n/2$, if n is even and $(n-1)/2$ if n is odd, and $\omega_j = (2\pi j/n)$ denotes frequency included in the cyclic fluctuation. Parameters A_j and B_j can be estimated by using the linear regression. More details on estimating the significant peaks of the periodograms are provided by Moreira et al. (2015).

Moreira et al. (2015) argued that considering drier months for periodicity might reflect the dryness which is insignificant for drought monitoring even though SPI-12 of dry month contains the effect of preceding 11 months. However, on the other hand, when we consider

the months with significant precipitation, SPI-12 values reflect a lack of precipitation in the previous months because more than 75% of rainfall occurs during the monsoon months in India. Therefore, in this study, all the drought indices have been used for only four monsoon months for detecting the hidden periodicities in the projected drought time series. Further, periodicity generally changes with time and space, so, the periodicity analysis has been performed for different time periods to calculate the temporal change in periodicities. Therefore, the periodicity analysis has been performed for three different time periods; Historical period (1951–2005), future period-1 (2020–2050) and future period-2 (2051–2100) to identify the changes in significant periodicities for these time periods.

3. Results and discussion

3.1. Identification of homogeneous drought regions

To identify the homogeneous drought-prone regions, drought characteristics such as average severity, duration and interval for each grid cell have been obtained using the historical gridded rainfall data for the period 1951 to 2005 based on the method of run approach. Therefore, for each grid cell, Latitude and Longitude of grid centre, average severity, duration and interval are used as the feature vectors for clustering. Values of DBI and ASWI have been examined for identifying the optimum number of clusters. Urcid and Ritter (2012) suggested checking the values of the validity indices for number of clusters varying from 2 to $\sqrt{n}$, therefore, values of ASWI and DBI have been examined by varying the number of clusters from 2 to 35 for 1232 feature vectors. Lower values of DBI and higher values of ASWI corresponds to well separated clusters, thus, optimum number of clusters are generally taken as the number at which DBI is minimum and ASWI is maximum. It can be noticed from Fig. 2 that both DBI and ASWI estimates indicate the optimum number of clusters as 2. However, considering only two homogeneous regions for the entire India is not justifiable on the physical considerations as Indian climate is very diverse and contains at least 6 sub-climatic zones (Bharati et al., 2001). Moreover, considering only two clusters will not serve the purpose of analysing spatial heterogeneity in the droughts. Therefore, for identifying the optimum number of clusters, second best values of DBI and ASWI have been examined. Second best value of the ASWI is for 9 clusters; however, it should be noted that the difference between the second and third best values (i.e. 10 clusters) is very less which suggests that the separation between clusters is almost similar for 9 and 10 clusters. Similarly, for DBI, the second best value is for 11 clusters and the difference between the separation of 10 and 11 clusters is approximately the same. Therefore, it is reasonable to select 10 as optimum number of clusters. Therefore, in this study, we considered 10 number of clusters as optimum number. Spatial analysis of the delineated clusters reveals that only 1, 6 and 1 grid points have been classified into Cluster 2, Cluster 3 and Cluster 4, respectively, therefore, these grid points have been merged with Cluster 9 which is the largest cluster in their vicinity as suggested by Hosking and Wallis (1993). Merged final clusters renumbered from 1 to 6 are shown in Fig. 3. Final formed clusters are showing broader resemblance with different climate zones in India and also with precipitation homogeneous regions used by Pattanaik (2007) and Parthasarathy et al. (1996).

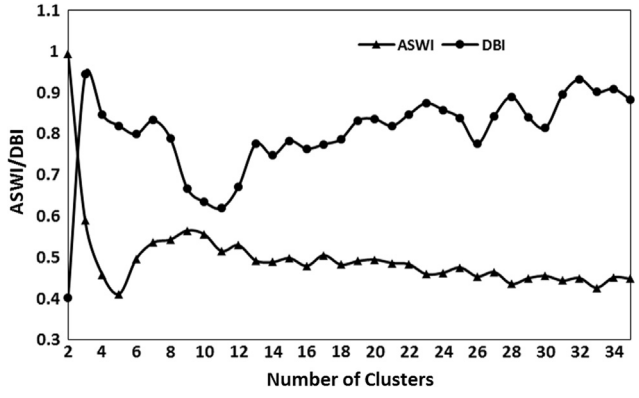

Fig. 2. Variation of Davies-Bouldin Index (DBI) and Average Silhouette Width Index (ASWI) for 2–34 clusters for K-means clustering.

Cluster 1 is mainly mountainous region with most of the area containing cold deserts of Jammu and Kashmir. The annual average historic (1951–2013) precipitation and temperature are 687 mm and 1 °C, respectively. Cluster 2 is the tropic wet climatic region which receives a very high average annual rainfall of 3167 mm with an average temperature of 25.6 °C. Cluster 3, which is southern Indian region falls under the semi-arid and tropical wet and dry climate class. The average annual temperature and precipitation for Cluster 3 are 868 mm and 26.6 °C respectively. Cluster 4, which consists of humid subtropic climatic region, is having an average annual precipitation and temperature values of 1276 mm and 25.6 °C. Cluster 5 is spread over the arid and the semi-arid climatic regions of India and receives an annual average rainfall of 704 mm with average temperature being 23 °C. Cluster 6 covers north-eastern parts of India which are characterized by humid subtropical climate and receives a high average annual precipitation of 2542 mm with an annual average temperature of 18.4 °C.

3.2. Performance evaluation of RCM models for drought simulation

Performance of various RCMs have been examined using Taylor diagram method. Fig. 4 shows the spatial Taylor diagram for performance comparison of seven RCMs and their ensemble average for the simulation of observed average monthly precipitation and temperature of past data in terms of their pattern correlation, root mean square difference (RMSD) and standard deviation. For precipitation simulation, spatial pattern correlation varies between 0.415 (for RCM5) and 0.682 (for RCM2). Correlation coefficient for ensemble average is found to be 0.656. However, best value of RMSD is found to be 49.75 for the ensemble average followed by the RCM2 with a value of 50.566. Further, RCM2 is found to have the nearest standard deviation of 64.579 as compared to 62.072 for the observed gridded precipitation. So, for precipitation simulation, RCM2 is found to be outperforming other models followed by ensemble average, RCM7, RCM6 and RCM1 etc. All RCMs simulate better pattern correlation for temperature than that of precipitation. RCM1, RCM2, RCM3 and RCM7 have been found to have correlation values in a very close range of 0.887 to 0.897. RCM2 is found to have minimum value of RMSD (5.024) thus representing the best performance compared to other RCMs. Further, for temperature simulation, RCM2 is also found to have the nearest values of standard deviation as compared to observed. Since, RCM2 performs better than other RCMs individually and their ensemble average for simulating precipitation and temperature. Therefore, RCM2 is selected for further analysis.

For the examination of spatial variability in average precipitation and temperature, spatial maps of precipitation and temperature has been prepared as shown in Fig. 5a(a). Fig. 5(b) shows the spatial distribution of precipitation and temperature bias for various parts of India. It was observed that RCM2 overestimates the precipitation mostly in drier regions of India such as Rajasthan, parts of Maharashtra, Andhra Pradesh, Telangana, Karnataka and Tamil Nadu. However, it underestimates the precipitation in high precipitation regions such as Western Ghats and Meghalaya in north-east of India. Model consistently underestimates the temperature values throughout India; however, higher underestimation up to 5–10 °C can also be observed for the Himalayan region as can be seen from Fig. 5(b) due to high variability of temperature in this region. To remove the bias in precipitation and temperature, many approaches for bias correction are available in the literature (Lenderink et al., 2007; Singh et al., 2017; Shivam et al.,

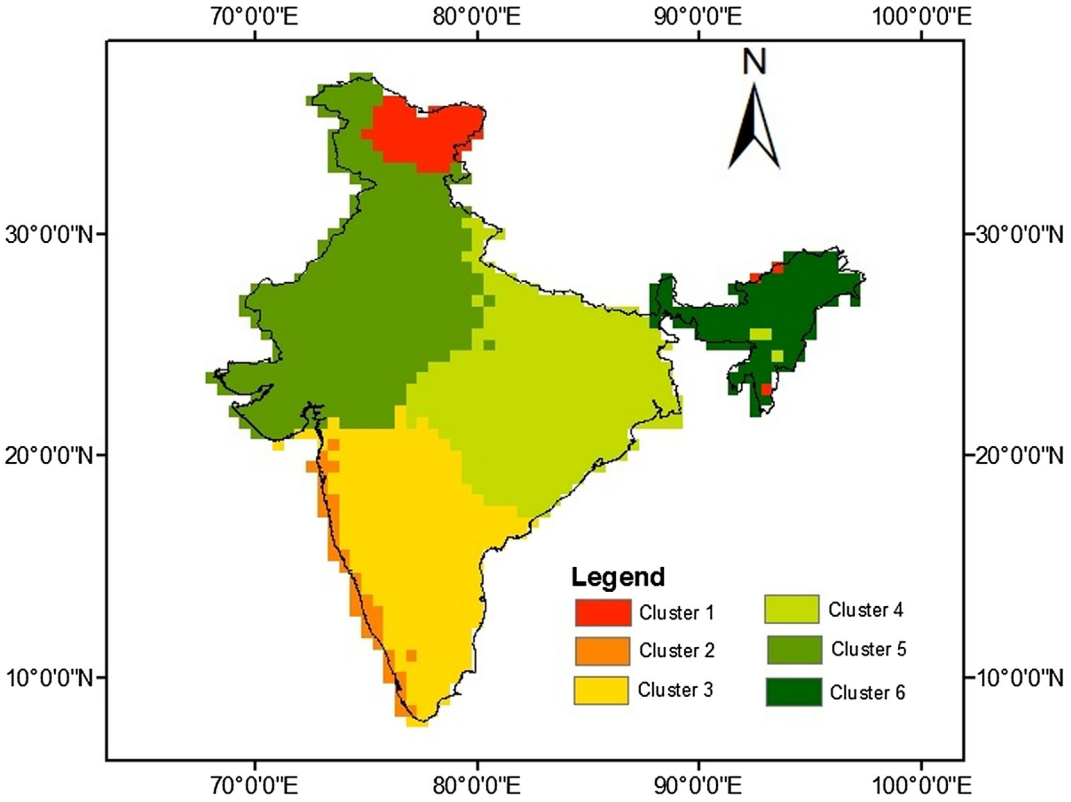

Fig. 3. Homogeneous drought clusters obtained by applying K-means clustering algorithm.

2017). For correcting the bias in data obtained from RCM, a linear bias correction (Lenderink et al., 2007) approach has been used for further analysis in this study. The time series of cluster averages of bias corrected precipitation and temperature with corresponding cluster averaged observed data has been shown in Figs. 6a and 6b. RCM2 simulates both the precipitation and temperature well for all the clusters except Cluster 1 for the case of precipitation. Low performance of simulated precipitation for Cluster 1 may be attributed to very small size of cluster and its mountainous topography.

Further, for examining the capability of RCM2 to identify important drought events, three drought indicators namely SPI, SPEI and SP*ETI have been estimated for the randomly selected points in each drought homogeneous clusters after correcting the bias in modelled temperature and precipitation. The comparison of three drought indicators for the modelled and observed climate in various homogeneous clusters is given in Fig. 7 as illustration. As it can be observed from Fig. 7 that the RCM2 is able to catch most of the major drought events in each cluster which indicate its capability toward simulating drought in various

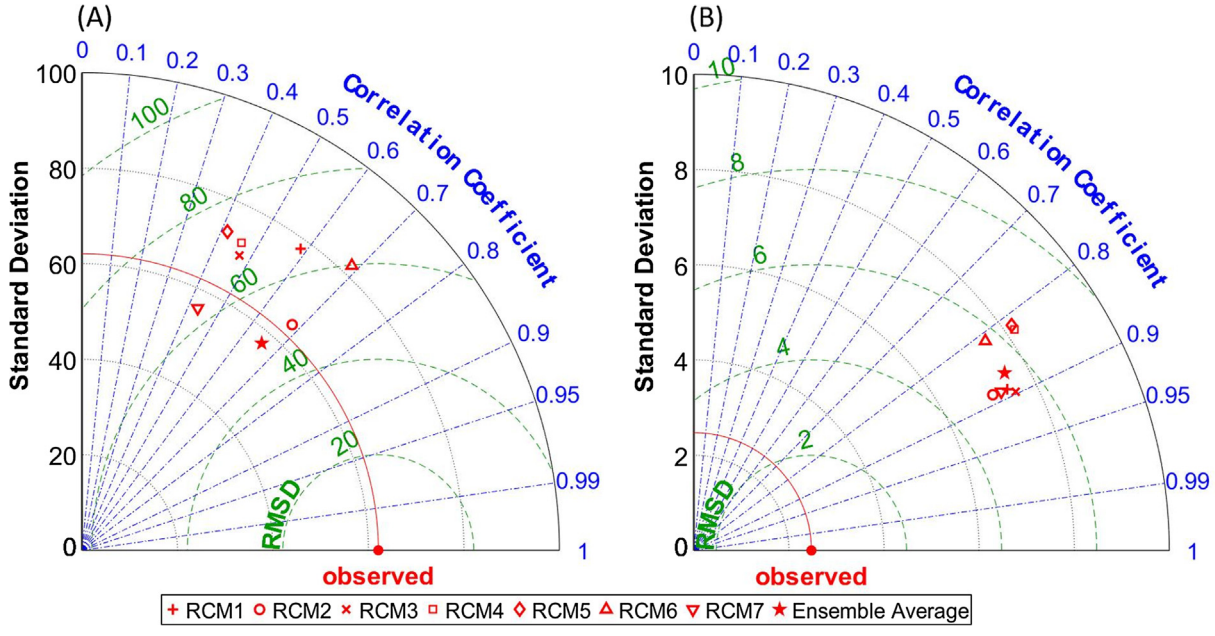

Fig. 4. Taylor diagram to examine performance of various RCM models for simulation of (A) precipitation and (B) temperature.

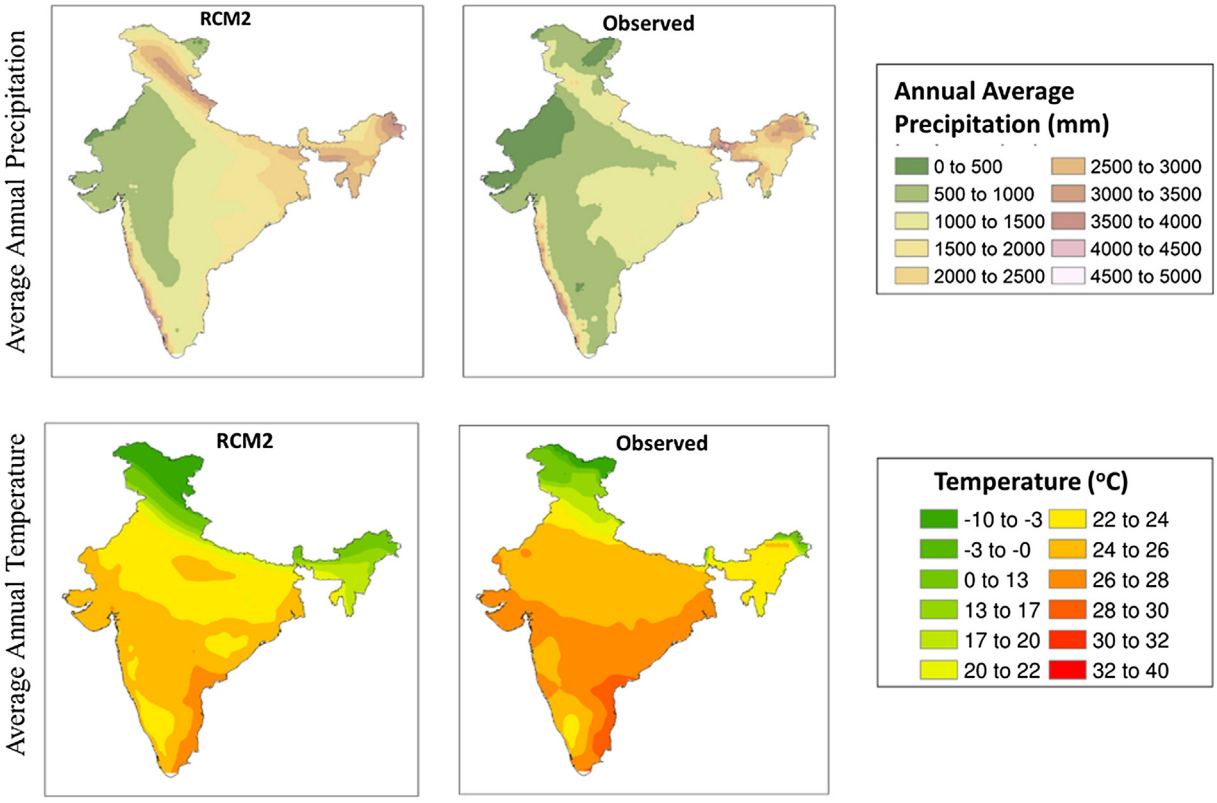

Fig. 5a. Spatial distribution of annual average precipitation (mm) and average temperature (°C) at each grid point.

regions of India.

Annual precipitation, temperature and potential evapotranspiration (PET) have been computed for each of the regions as shown in Fig. 8. Temperature and PET are found to have increasing trend for all the clusters under both the RCPs as shown in Table 2. Precipitation is also projected to have an increasing trend for Cluster 1, 2 and 3 under both the scenarios. However, for Cluster 4, a significant increasing trend has been projected for only the RCP 8.5. Further, under the RCP 4.5, projected Sen's slope for PET is found be higher than of the precipitation for all the clusters, except Cluster 2 and 6. For the RCP 8.5, the rate of change of PET is significantly higher than rate of change of precipitation for all except that of Cluster 2 for which the rate of increase in precipitation is of very higher order.

3.3. Trends in severity and frequency of droughts

Drought characteristics such as the severity and frequency have been estimated for each grid point as described in section 2.5 for the SPI, SP*ETI and SPEI series. Modified Mann-Kendall and Sen's slope test have been performed on the computed series of annual drought severity and frequency at each grid point for the period 1951 to 2100 by dividing total periods in three sub periods; Historical period (Hist, 1951–2005), Near Future (NF, 2021–2050) and Far Future (FF, 2071–2100). The results obtained for both the tests are shown in

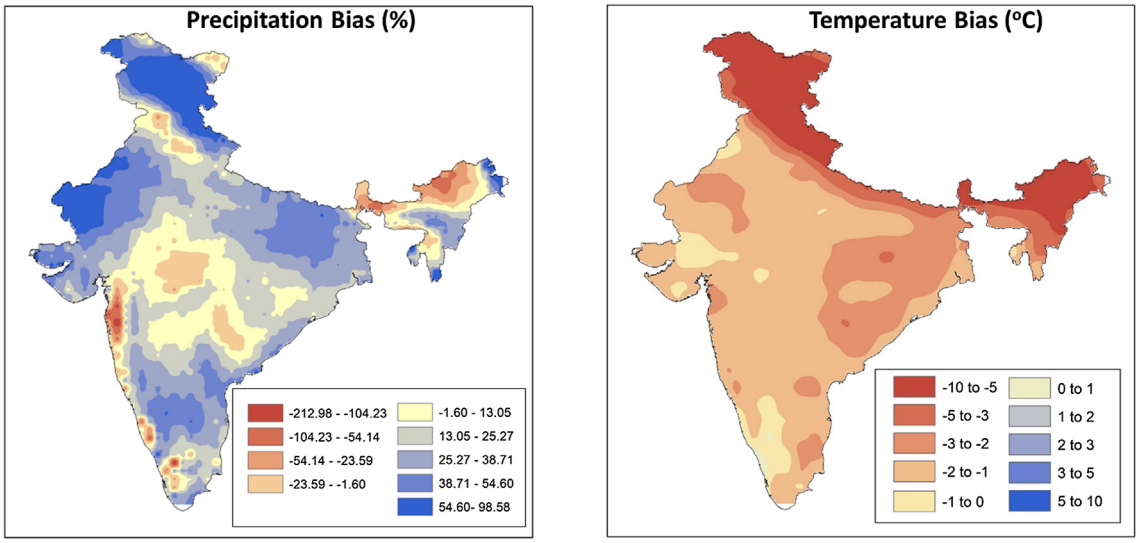

Fig. 5b. Spatial distribution of precipitation and temperature bias over a period of 1951–2005 for RCM2 model.

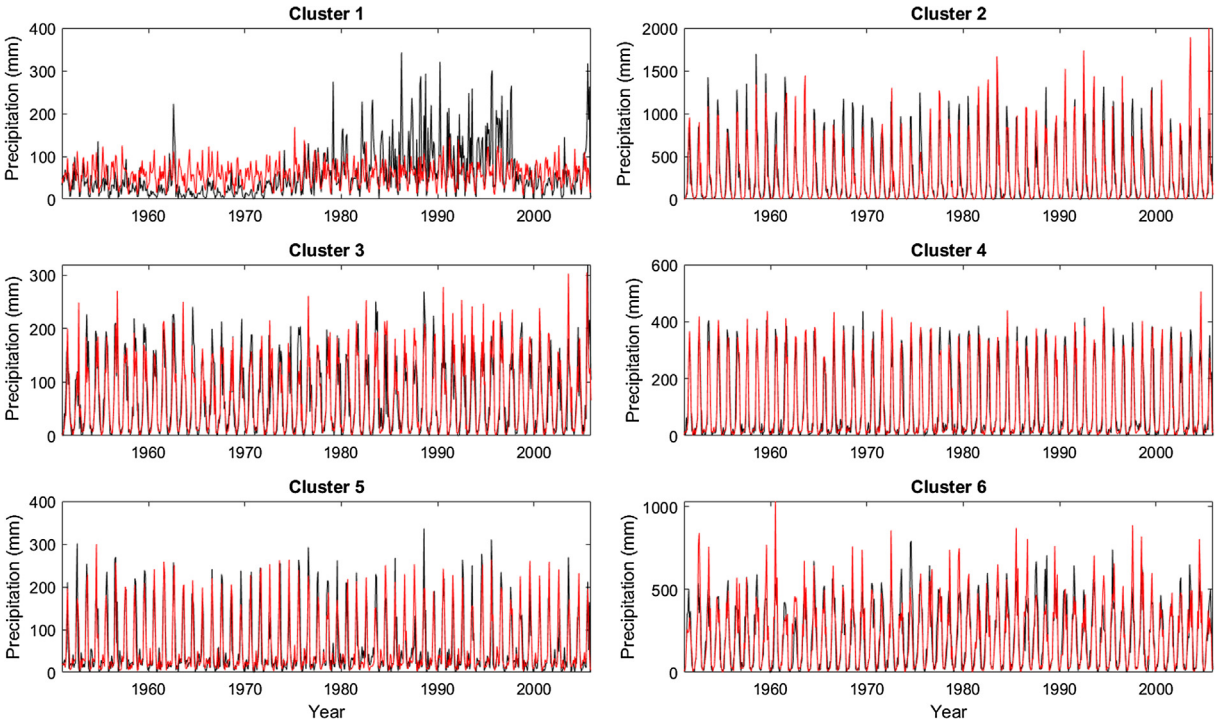

Fig. 6a. Comparison of cluster averages of observed precipitation and bias corrected precipitation of RCM2 for various clusters.

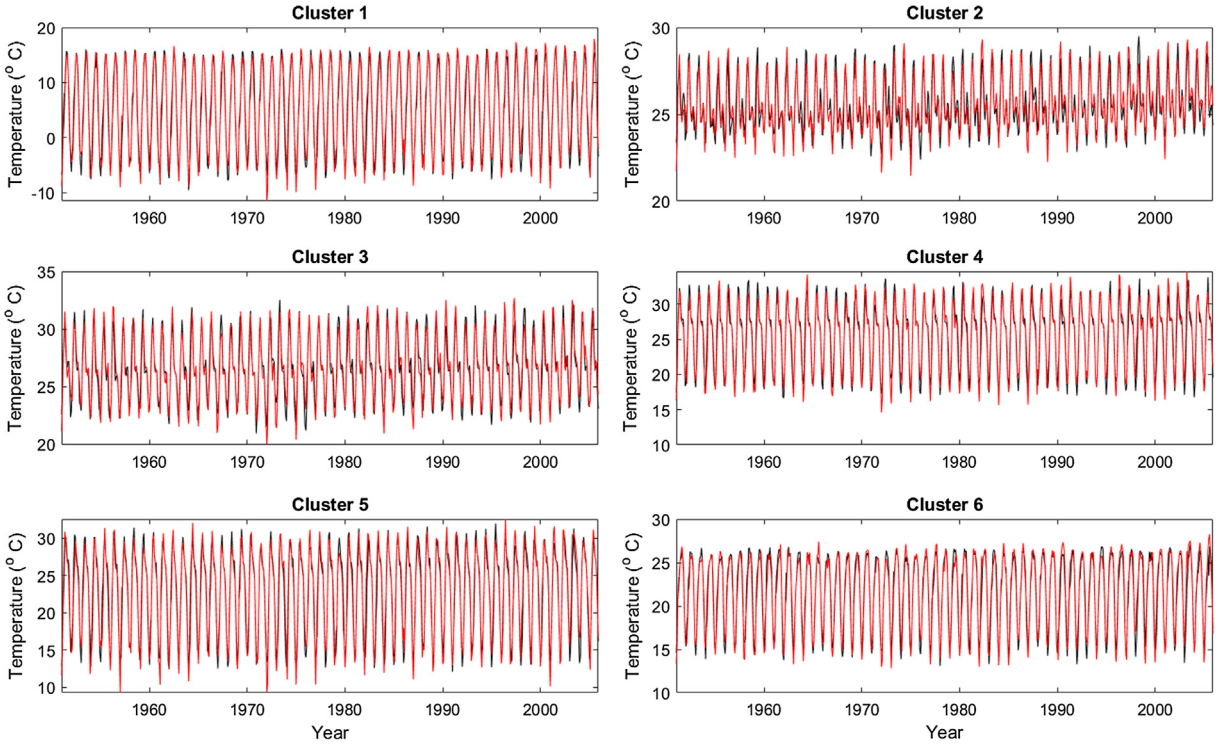

Fig. 6b. Comparison of cluster averages of observed and bias corrected temperature of RCM2 for various clusters.

Figs. 9a, 9b and 9c. Severity values multiplied by -1 have been used to get the positive trends for the increasing drought severity and vice versa. Average values of the Sen's slope for drought, severity and frequency are shown in Table 3 and the spatial distribution of Sen's slope and modified Mann-Kendall tests are shown in Figs. 9a, 9b and 9c.

For Cluster 1 (i.e. Jammu and Kashmir) almost all drought indices project a decreasing trend in severity and frequency under the RCP 4.5 for all three analysed periods. However, for RCP 8.5, drought severity obtained from the SPI shows decreasing trend whereas both the precipitation-evapotranspiration based drought indices show an increasing trend in Cluster 1 for NF and FF period indicating a significant impact of ET on drought occurrence in this region. Cluster 2 (i.e. Western Ghats) shows a positive average Sen's slope of severity and frequency for the historical period as well as for both the future periods under RCP 4.5. However, under RCP 8.5, a decline in overall slopes of severity and frequency is projected for NF period which may escalate in the FF

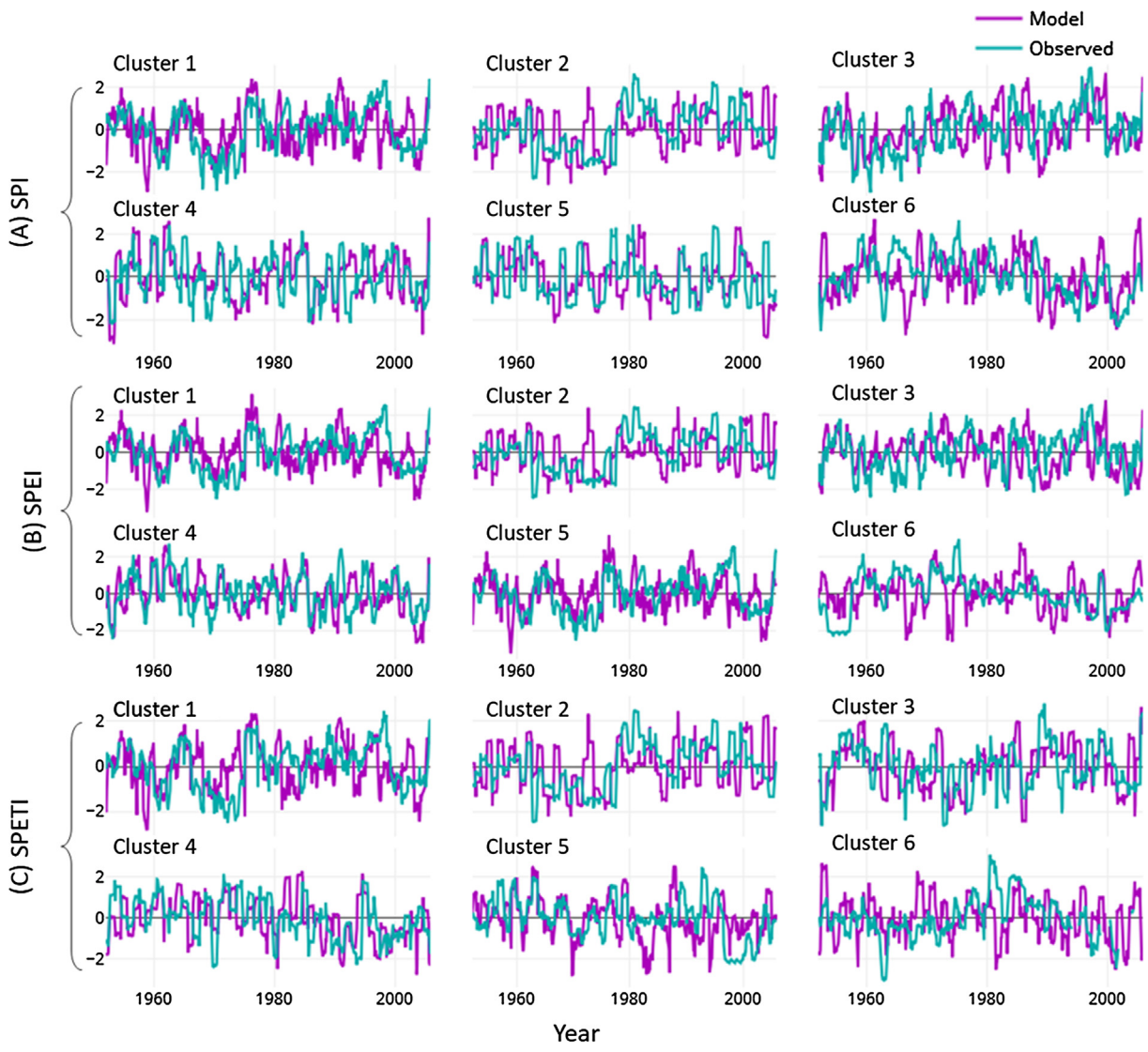

Fig. 7. Comparison of Drought indices computed for observed climate and RCM2 model generated climate at random points in each cluster.

period. Cluster 3 i.e. the southern Indian region shows an increasing trend in drought severity and frequency for historical droughts for all the drought indicators. The modified Mann-Kendall and Sen's slope tests suggest decreasing trends in severity and frequency for SPI under both the concentration pathways during both NF and FF periods. However, increasing trends in severity and frequency in northern parts of Cluster 3 (Maharashtra, Telangana, and Chhattisgarh etc.) are projected for both the evapotranspiration-based drought indices under the RCP 4.5, whereas, increasing trends can be observed for almost the whole cluster 3 for the RCP 8.5.

For Cluster 4 which consists of central and eastern states such as Uttarakhand, parts of Uttar Pradesh (UP), Chhattisgarh, parts of Madhya Pradesh, Jharkhand, Bihar and Odisha, the average Sen's slope values for drought severity and frequency have been found to have an increasing trend which may continue under RCP 4.5 for the near future (NF). For the West Bengal region of this cluster, decreasing trends in drought severity and frequency have been observed in the past which are also expected to continue for the RCP 4.5. Further, for FF, under RCP 4.5, drought intensification is expected to take place since drought severity is projected to increase and drought frequency is expected to decrease in this region. For Cluster 5, both the evapotranspiration-based drought indices suggest a likeliness of increasing trends in drought severity and duration under both the RCPs for all analysed periods, including the historical period. It is noteworthy that the average slope values for the FF period are marginally higher for RCP 8.5 than for RCP 4.5 which suggests a significant impact of GH concentration in this region for far future. Further, SPI index shows a decreasing trend in drought severity and frequency for the FF period in cluster 5 which may be attributed to the projected increase in monsoon precipitation in FF. Cluster 6 which consists of North-eastern states of India shows decreasing trends in drought severity and frequency for FF for all the drought indicators under the RCP 4.5. Projected SPI exhibits an average decreasing slope of drought severity and frequency for the RCP 8.5. However, other two evapotranspiration based indices indicate a possibility of increasing trend for both the NF and FF periods.

Overall, for the historic droughts, similar pattern of significant trends have been observed for all the drought indices which suggests increasing trends in drouht severity and frequency over the northen states such as Punjab, Haryana, Rajasthan and Uttar Pradesh and over almost all the southern Indian states. However, decreasiging trends have been observed over the Jammu and Kashmir region, west Bengal, Bihar and Northeastern states for historic droughts. For the RCP 4.5, increasing trends of drought severity and frequency are mostly distributed around the central and western states in the near future (NF). However, for far future (FF) a spatial southward shift can be seen in increasing trends. For the regions strtetching from Rajasthan to Andhra

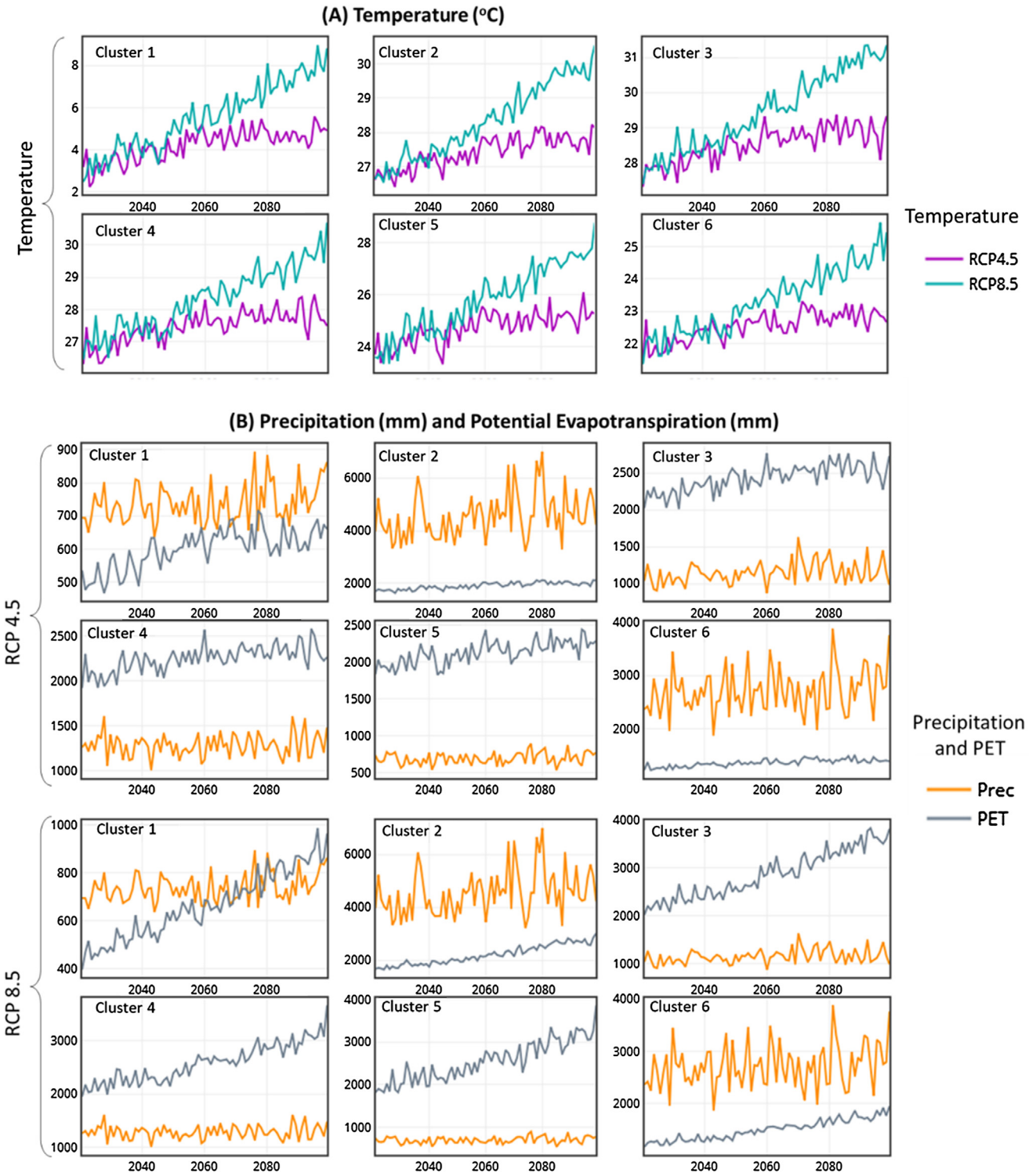

Fig. 8. Temporal variation of cluster averages of projected (A) temperature (°C) (B) precipitation (Prec; mm) and potential evapotranspiration (PET; mm) under RCP 4.5 and RCP 8.5.

pradesh including the parts of Madhya Pradesh, Maharashtra, Chattisgarh, Telangana and Odisha, drought severity and frequency are expected to increase in FF which can be attributed to the dominance of evapotranspiration on droughts in these regions which is rising due to the increase in temperature. Under the RCP 8.5, the drought escalating trends are mostly concentrated to western parts of the country in the NF period. However for the FF period, evapotranspiration is projected to have pronounced effects on droughts since values of SPEI shows higher magnitude of increasing trends in most parts of the country under the RCP8.5. In FF under the RCP 8.5, droughts are expected to decrease in eastern parts of the country such as Odisha, Chattisgarh and Telangana. However, for the rest of the country droughts are likely to escalate quickly during this period.

Table 2
Results of modified Mann-Kendall and Sen's slope test for projected precipitation, temperature and PET. 1, 0 and −1 represent a significantly increasing trend, no significant trend, and significantly decreasing trends.

	Sen's slope					
	Precipitation		Potential Evapotranspiration		Temperature	
	RCP 4.5	RCP 8.5	RCP 4.5	RCP 8.5	RCP 4.5	RCP 8.5
Cluster 1	0.666	1.521	1.939	5.767	0.024	0.067
Cluster 2	11.105	32.247	4.523	15.103	0.017	0.046
Cluster 3	1.573	2.928	6.090	20.553	0.018	0.047
Cluster 4	0.214	2.056	4.211	14.288	0.016	0.040
Cluster 5	0.710	0.103	4.773	18.426	0.019	0.055
Cluster 6	3.538	2.988	2.236	7.738	0.015	0.041
	Modified Mann-Kendall's test					
Cluster 1	1	1	1	1	1	1
Cluster 2	1	1	1	1	1	1
Cluster 3	1	1	1	1	1	1
Cluster 4	0	1	1	1	1	1
Cluster 5	0	0	1	1	1	1
Cluster 6	0	0	1	1	1	1

3.4. Analysis of annual minimum SPI, SP*ETI and SPEI

Temporal variation in regional (cluster) average values of SPI, SP*ETI and SPEI have been analyzed using annual minimum SPI, SP*ETI and SPEI values obtained from an averaged series estimated by spatially averaging the monthly SPI, SP*ETI and SPEI values for the grids falling in a cluster as shown in Fig. 10. Results of the modified Mann-Kendall trend test of Annual minimum SPI, SP*ETI and SPEI are summarized in Table 4. It can be observed from Figs. 10(B) and 8(C) that the SPEI indicates lesser drought intensity (annual minimum drought index value) in the first half of the century for most of the clusters except Cluster 2 and 6. However, the SPI index shows more droughts intensity in the first half of the century than that of the second half of the century. Difference in drought intensities represented by the drought indicators is higher for the extreme scenario of RCP 8.5 than that of RCP 4.5. Higher drought intensities shown by the SPI in the first half and SPEI in the second half suggest that the cause of droughts in the first half of the century is attributed to precipitation deficit; however, in the second half of the century, it is due to the increase in evapotranspiration owing to the rise in temperature. Further, for Cluster 2 (Western Ghats) and Cluster 6 (Northeast India), all the indices show a high correlation with each other and almost similar values throughout the century. This can be attributed to a high precipitation in these regions that could probably eclipse the effect of rise in evapotranspiration due to climate change in these regions thus negating the effect of increase in evapotranspiration for drought formation.

From Table 4, it can be observed that for the Cluster 1, the annual minimum SPEI shows a significant decreasing trend under the RCP 8.5 for the NF. However, no such significant trends could be envisaged for the FF. Also, a decreasing overall trend has been projected for both the ET based drought indices which can be attributed to the rate of change of PET being more than the rate of change of precipitation. In the NF, a negative trend is projected for the cluster 2 under the RCP 8.5 which suggests an increase in the drought intensity. However, an overall

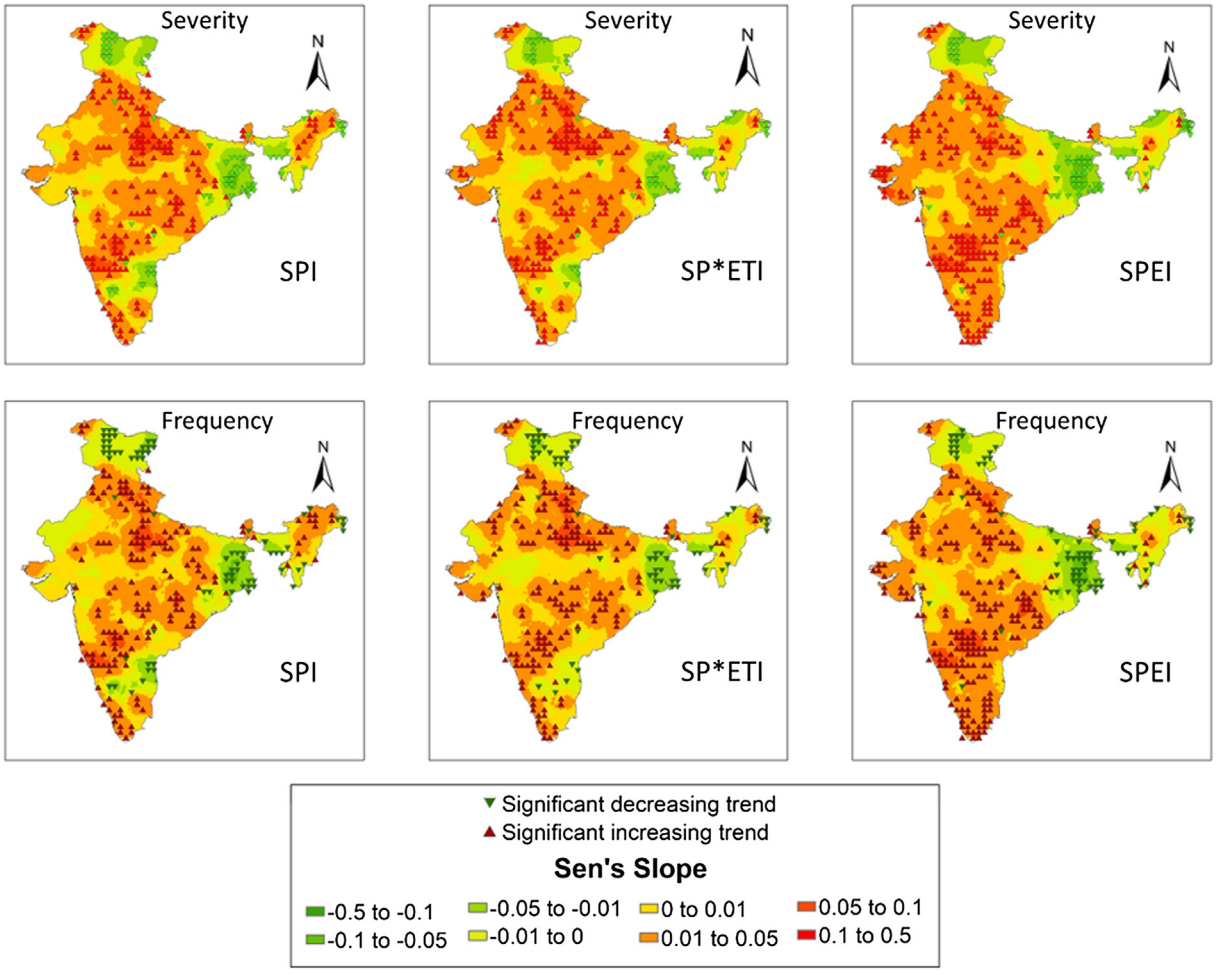

Fig. 9a. Mann-Kendall and Sen's Slope test results for drought severity and frequency for historic droughts for SPI, SP*ETI and SPEI drought indicators.

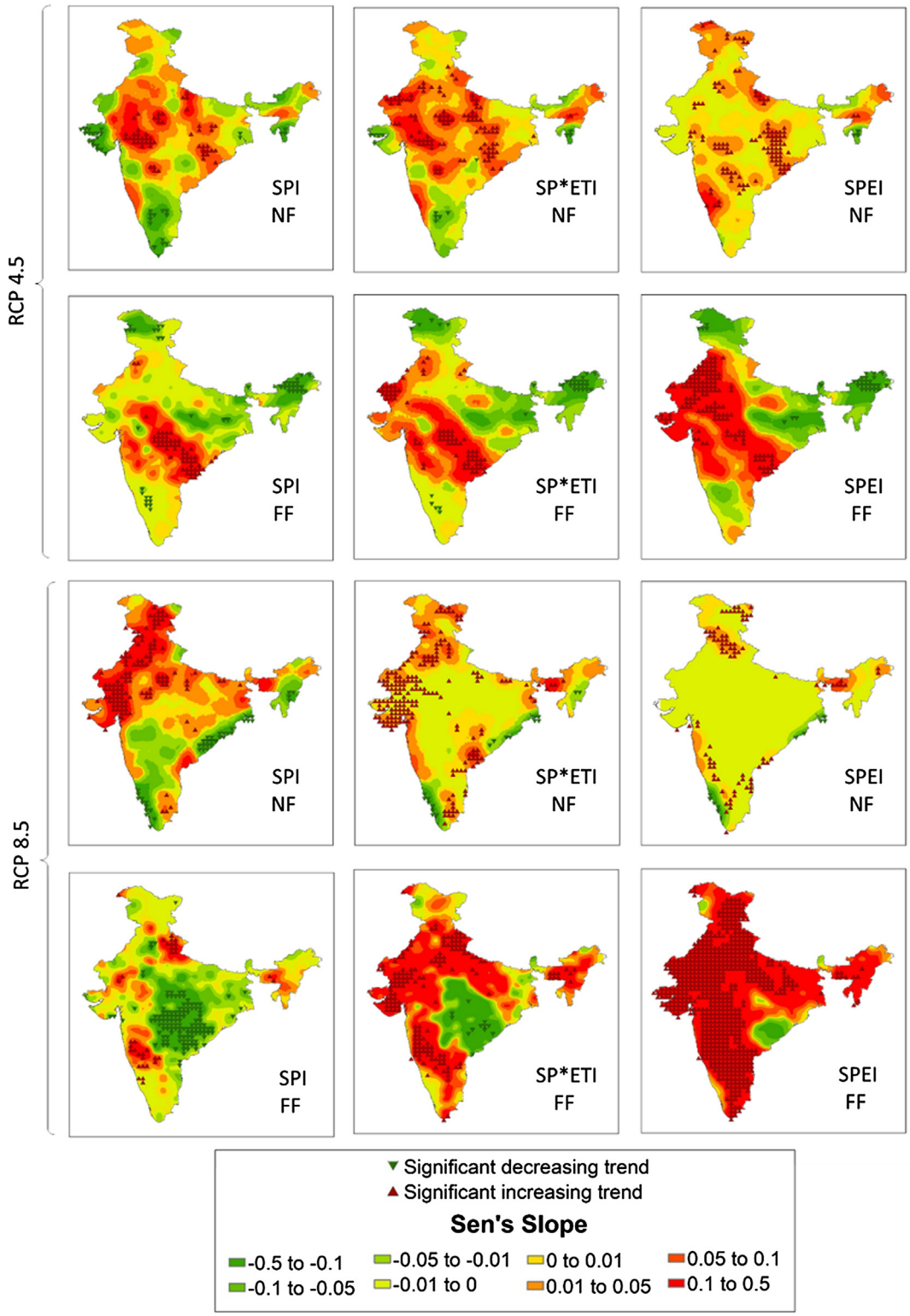

Fig. 9b. Mann-Kendall and Sen's Slope test results for drought severity for near future (NF) and far future (FF) for SPI, SP*ETI and SPEI drought indicators.

increasing trend of drought indices for the period 2021–2100 is likely possible which indicates a decreasing trend in the drought intensities. Cluster 3 shows a significant increasing trends in drought intensities under the higher temperature change only. Drought intensities may decrease for short periods in the NF and FF under the RCP 8.5; however, an overall increasing trend can be expected in drought severity since DIs show decreasing trends in Cluster 3. For Cluster 4, the SPEI and SP*ETI are found to have an overall negative trend, thus, representing an increase in droughts over this region. Cluster 5, which includes mostly drier region of India, is expected to experience a decreasing trend in drought intensities for a short term in the NF. However, for a long-term period of 2021–2100, increasing trends in drought intensities can be expected for this region. For the Cluster 6, no significant trends have been observed for the NF and FF; however, a decreasing trend of SPEI is expected under the RCP 8.5.

All the indicators have been found to project different drought peaks

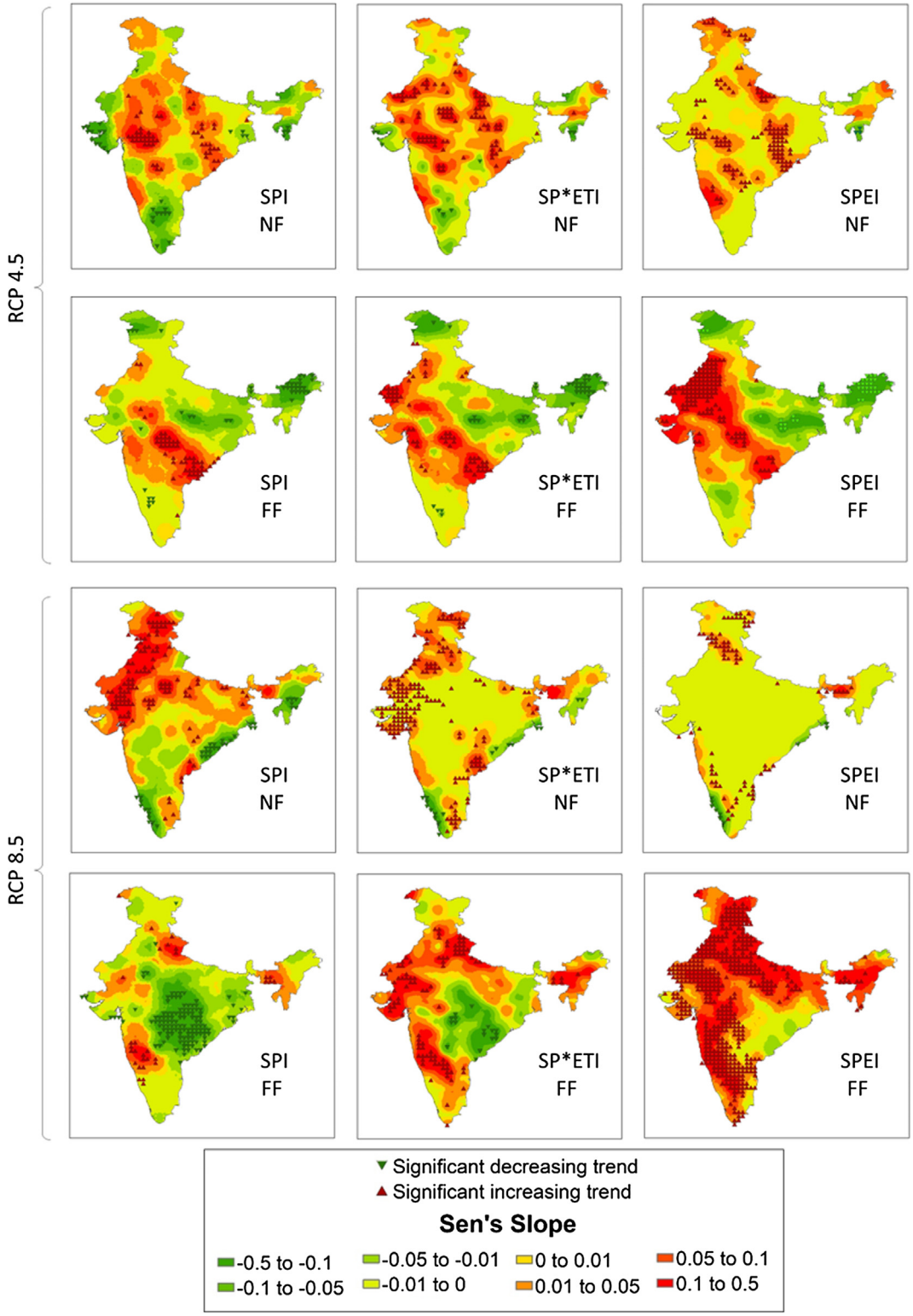

Fig. 9c. Mann-Kendall and Sen's Slope test results for Drought Frequency for near future (NF) and far future (FF) for SPI, SP*ETI and SPEI drought indicators.

for different time periods under different RCP scenario, but, common incidences such as drought peak in 2060 and 2080 can also be noticed. Further, it is important to notice that a sudden fall in the drought indicator values could be observed after the year 2050 for Cluster 3, 4 and 5, thus, indicating a possibility of droughts becoming severe for these clusters.

3.5. Analysis of the areal extent of drought affected area with time

The extent of the drought-affected area at a given instance of time – for each of the clusters and India as a whole – defined as the ratio of the area of the grid cells exhibiting the SPI, SP*ETI or SPEI indices value below −0.5 to the total area of all the grids falling into the region of interest have been computed for the RCP4.5 and RCP8.5, and the same

Table 3
Average value of Sen's Slope of average annual severity and frequency for different clusters for historical period (Hist), near future (NF; 2021–2050) and far future (FF; 2071–2100).

			Cluster 1		Cluster 2		Cluster 3		Cluster 4		Cluster 5		Cluster 6	
		Time period	Sev	Freq	Sev	Freq	Sev	Freq	Sev	Freq	Sev	Freq	Sev	Freq
SPI	Historical	Hist	−0.017	−0.009	0.019	0.017	0.014	0.013	0.009	0.007	0.018	0.014	0.003	0.007
	RCP 4.5	NF	−0.017	−0.013	0.017	0.029	−0.029	−0.017	0.024	0.019	0.019	0.013	−0.031	−0.037
		FF	−0.045	−0.034	0.005	0.003	0.041	0.032	0.010	−0.002	0.003	0.001	−0.078	−0.078
	RCP 8.5	NF	0.091	0.088	−0.109	−0.086	−0.016	−0.007	−0.009	−0.005	0.094	0.077	−0.001	−0.015
		FF	−0.002	−0.002	0.000	0.000	−0.015	−0.012	−0.077	−0.066	−0.001	−0.003	0.015	0.015
SP*ETI	Historical	Hist	−0.016	−0.008	0.015	0.017	0.015	0.014	0.013	0.009	0.019	0.015	−0.001	0.002
	RCP 4.6	NF	−0.007	−0.006	0.038	0.032	0.002	0.006	0.033	0.028	0.045	0.034	0.003	−0.011
		FF	−0.082	−0.063	0.005	0.002	0.059	0.035	0.010	−0.004	0.026	0.023	−0.104	−0.092
	RCP 8.6	NF	0.034	0.039	−0.076	−0.077	0.010	0.008	−0.006	−0.002	0.015	0.016	0.023	0.016
		FF	0.022	0.004	0.005	0.005	0.095	0.035	−0.015	−0.023	0.166	0.063	0.063	0.047
SPEI	Historical	Hist	−0.021	−0.008	0.020	0.019	0.029	0.028	0.004	0.002	0.023	0.017	−0.010	0.001
	RCP 4.6	NF	0.017	0.017	0.042	0.033	0.017	0.018	0.015	0.019	0.009	0.009	0.007	−0.003
		FF	−0.104	−0.052	0.009	0.007	0.058	0.019	0.014	−0.007	0.140	0.097	−0.130	−0.115
	RCP 8.6	NF	0.001	0.001	−0.065	−0.062	0.001	0.001	−0.006	−0.004	0.002	0.003	0.016	0.013
		FF	0.329	0.119	0.056	0.026	0.362	0.073	0.172	0.060	0.425	0.105	0.131	0.082

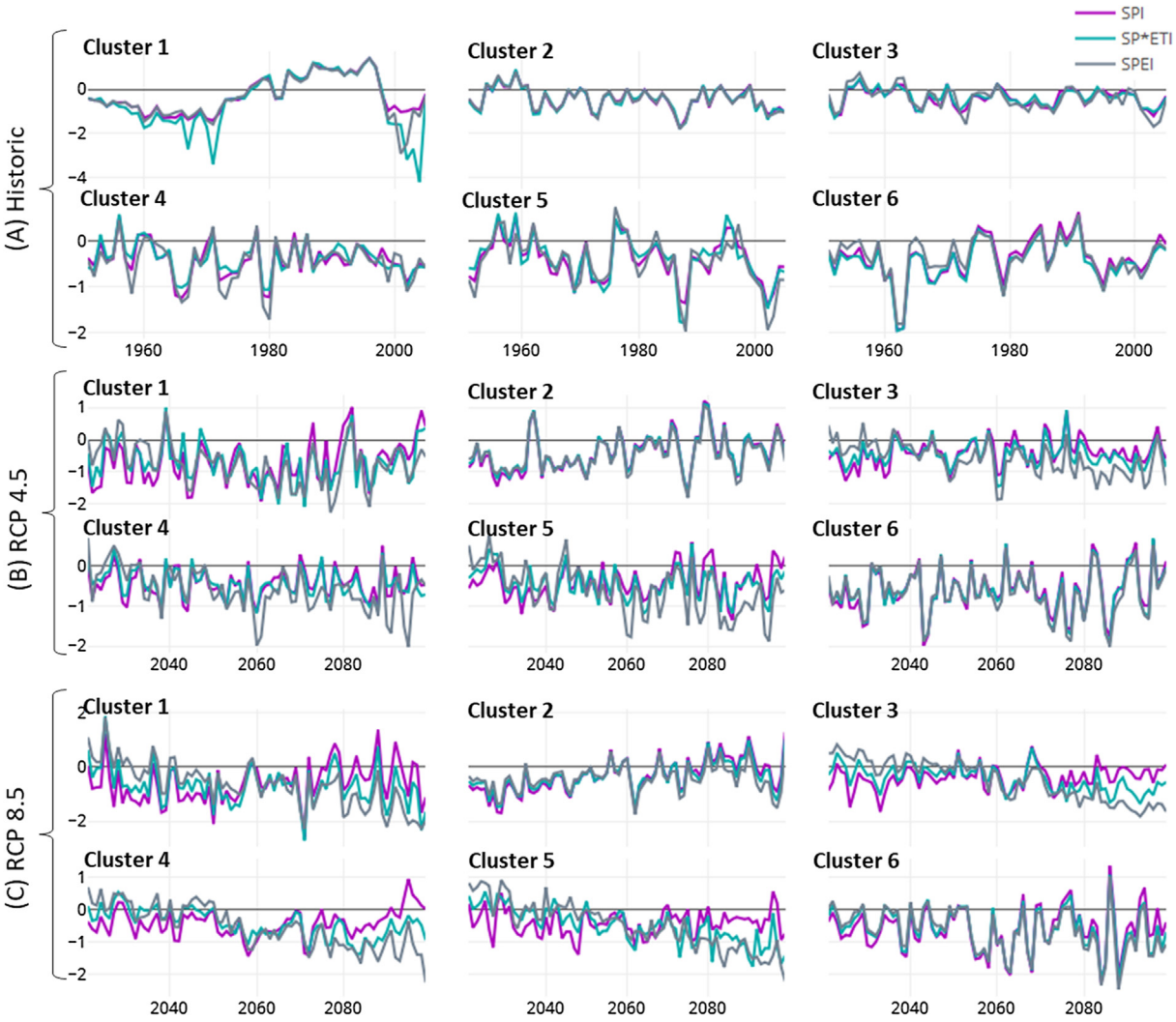

Fig. 10. Temporal variation of annual minimum SPI, SP*ETI and SPEI for 21st century.

has been plotted as shown in Fig. 11. The Modified Mann-Kendall trend test on the maximum annual drought-affected areas has also been performed to identify the statistically significant trends. Results of trend analysis are presented in Table 5. Fig. 11 also shows the temporal extent of drought-affected areas as the percentage of the total area falling in different clusters for RCP4.5 and RCP8.5. As can be seen from Fig. 11, all the drought indicators show a higher correlation for the time series of annual maximum drought affected areas under the RCP 4.5 than that

Table 4
The result of Mann-Kendall and Sen's Slope trend test of Annual minimum SPI, SP*ETI and SPEI for near future, far future and total future. 1, 0 and −1 stand for a significantly increasing trend, no significant trend, and significantly decreasing trends.

	RCP	Cluster 1			Cluster 2			Cluster 3			Cluster 4			Cluster 5			Cluster 6		
		NF	FF	TP	NF	FF	TP	NF	FF	TP	NF	FF	TP	NF	FF	TP	NF	FF	TP
SPI	RCP 4.5	0	0	0	0	0	1	0	0	0	0	0	0	0	0	0	0	0	0
	RCP 8.5	0	0	1	−1	0	1	0	0	0	0	−1	0	1	0	0	0	0	0
SPETI	RCP 4.5	0	0	0	0	0	1	0	0	0	0	0	−1	0	0	0	0	0	0
	RCP 8.5	0	0	−1	−1	0	1	0	0	−1	0	0	−1	1	1	−1	0	0	0
SPEI	RCP 4.5	0	0	−1	0	0	0	0	0	−1	1	0	−1	1	0	−1	0	0	0
	RCP 8.5	1	0	−1	0	0	0	1	1	−1	0	0	−1	0	1	−1	0	0	−1

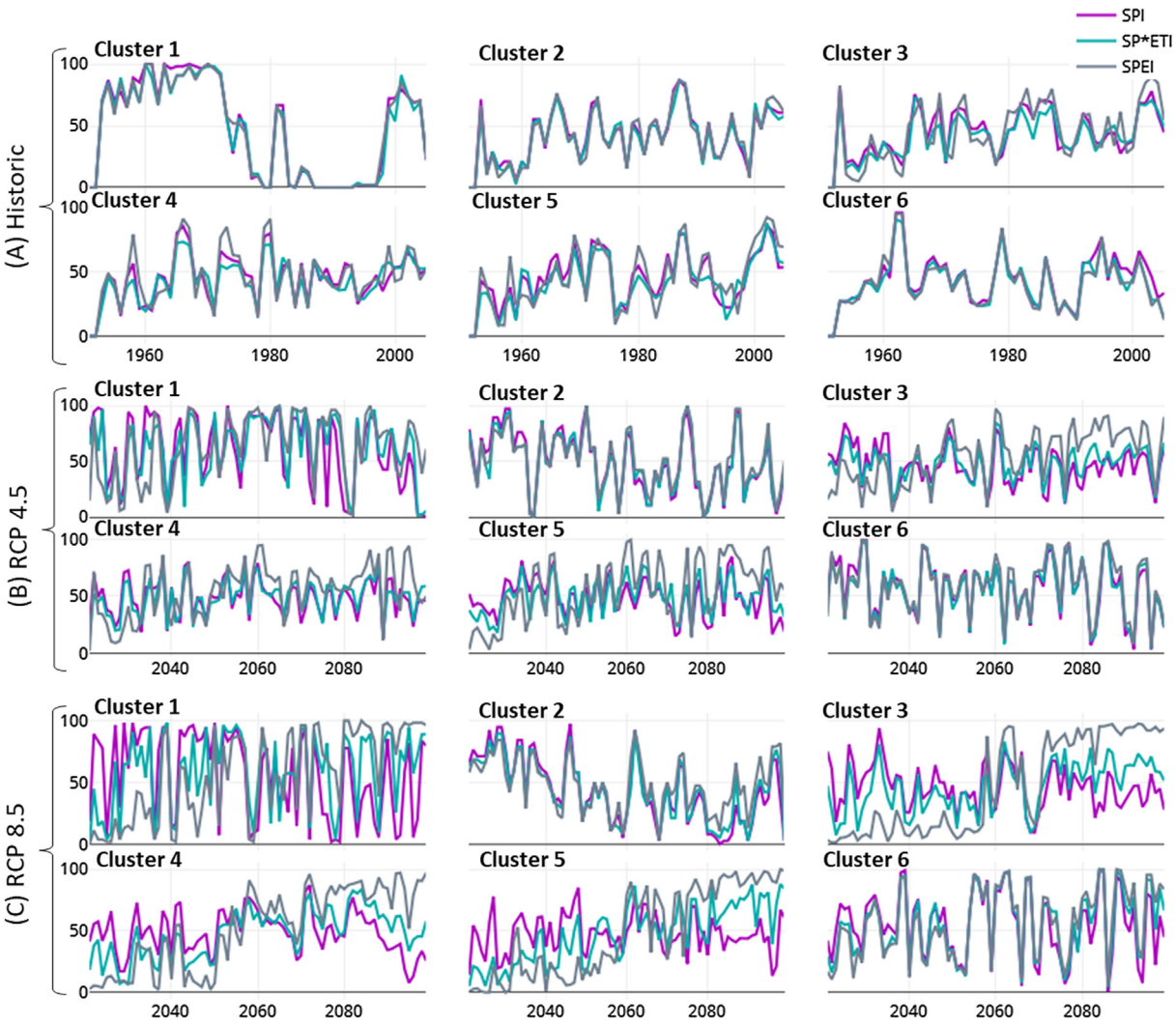

Fig. 11. Temporal variation of annual maximum drought affected area using SPI, SP*ETI and SPEI for 21st century.

of the RCP 8.5 which indicate that the temperature change may significantly affect larger areal extent under the RCP 8.5. Also the effect of ET on the projected droughts is likely to be more dominant, especially in Clusters 3, 4 and 5 under the RCP8.5. During the second half of the 21st century, the SPEI projects a substantial increase in the drought-affected area compared to the other two indices. For the RCP 8.5, it is interesting to notice that the SPI projects larger drought-affected area in the first half of the 21st century for almost all the clusters and smaller drought affected areas in the second half of the century as compared to the SPEI. The maximum drought affected area computed using the SPI shows decreasing trend at a higher rate for the RCP8.5 than that for the RCP4.5 which indicates that the precipitation based drought affected area may decrease at a higher rate under the extreme greenhouse gas concentration pathway. However, the drought affected areas computed by the other two drought indices considering the ET in the computation show that the widespread droughts are expected under the RCP 8.5 for the second half of the century highlighting the impact of temperature change in the development of droughts in various regions of India.

The projected extent of the area under severe droughts for the Cluster 2 is found to be decreasing for the SPI and SP*ETI under both the RCPs; whereas, for the SPEI, significant increasing trends in the drought affected areas have been found. Clusters 3, 4 and 5 are found to

Table 5
The results of modified Mann-Kendall test of the maximum annual drought-affected area. 1, 0 and −1 represent a significantly increasing trend, no significant trend, and significantly decreasing trends.

	RCP	Cluster 1			Cluster 2			Cluster 3			Cluster 4			Cluster 5			Cluster 6		
		NF	FF	TP	NF	FF	TP	NF	FF	TP	NF	FF	TP	NF	FF	TP	NF	FF	TP
SPI	RCP 4.5	0	0	0	0	0	−1	0	0	0	0	0	0	0	0	0	0	0	0
	RCP 8.5	0	0	−1	−1	0	−1	0	0	0	0	−1	0	1	0	0	0	0	0
SP*ETI	RCP 4.5	0	0	0	0	0	−1	0	0	0	0	0	1	0	0	0	0	0	0
	RCP 8.5	0	0	0	−1	0	−1	0	0	1	0	0	1	1	1	1	0	0	0
SPEI	RCP 4.5	0	0	1	0	0	0	0	0	1	1	0	1	1	0	1	0	0	0
	RCP 8.5	1	0	1	0	0	0	1	1	1	0	0	1	0	1	1	0	0	0

have significantly increasing trends in the maximum annual drought-affected area for both the ET based drought indicators (i.e. SP*ETI and SPEI) which can be attributed to the dominance of ET over precipitation in these regions.

3.6. Mapping of spatial variability of drought hazard

Drought characteristics obtained using the indices SPI, SP*ETI and SPEI under the RCP 4.5 and 8.5 have been further post-processed to compute the DHI using Eq. (4). For the estimation of weights used in Eq. (4), a value of 1, which represents the equal importance for all the sub-indicators has been taken while calculating the eigenvalues and the eigenvectors of the square preferential matrix of Analytical Hierarchical Processing (AHP; Saaty, 1977). Maccioni et al. (2014) also suggested to give equal importance to sub-indicators such as frequency, duration and magnitude while computing drought hazard index. Weights of each sub-indicator is found to be 0.25 from the AHP analysis. Fig. 12 shows the spatial distribution of drought hazard index for different drought indices and RCPs. Since the sub-indicators have been assigned scores, varying from 1 to 4 based on the threshold values, the DHI values also vary between 1 and 4 where 1 represents a least drought hazard and 4 represents a highest drought hazard. Threshold values for all sub-indicators are obtained by equally dividing the number of events in all the drought events generated by all the indicators under all the scenario for better comparability among the Drought indices and RCPs.

It is interesting to notice from Fig. 12 that the SPEI projects the highest drought hazard as compared to the other two drought indicators which suggests that considering evapotranspiration at potential rate results in projection of more drying leading to more projected drought risk. Further, the spatial variability of the DHI values for all the drought indices estimated for the historical period are found to be smaller as compared to the DHI estimated for the future under both the RCPs. As it can be observed from Table 6 that for each of the clusters, all the drought indices estimate similar values of hazard for the historical period which suggests that for the historical period considered in this study, a rise in temperature, if any, has not altered the evapo-transpiration in a significant way to influence the drought characteristics estimated using the ET based drought indicators SPEI and SP*ETI. However, during the future time periods, the dominance of evapotranspiration can be observed from the fact that cluster averages of the DHI for SPEI are marginally higher than the other two drought indices. The estimate of SPI projects lesser drought hazard for all the clusters except for clusters 4 and 6 which implies that a higher emission concentration may decrease the precipitation-based drought hazard. However, both precipitation and evapotranspiration-based indices show an escalated drought hazard for the RCP 8.5. The spatial distribution of DHI indicates the likelihood of severe drought hazard in central India for the RCP 4.5 which is likely to escalate with an increase in the evapotranspiration. However, for the RCP 8.5 the area with severe drought hazard is likely to increase and a shift towards south-eastern states is also expected.

3.7. Periodicity of droughts

Periodicity analysis of droughts for the monsoon months has been carried out using the Fourier analysis. Significant periodicities, which are above 90% confidence interval, have only been considered. Periodograms of SPI, SP*ETI and SPEI series have been calculated for examining the hidden cycles of drought in different clusters for all the four monsoon months for each grid point across all over India. For analysing the change in periodicity over time, three-time periods, historic (1951–2005), future period 1 (2020 to 2050) and future period 2 (2051 to 2100) have been used. Fig. 13 summarizes the results of significant peaks of the periodograms averaged over four months for different clusters and as well as for the whole India. It is inferred from this figure that in general, the percentage of area for all the significant peaks, and for all the clusters and time periods exhibits almost similar values implying least impact of climate change on the periodic cycles of drought in India. Periodicities of the order of 2 years to 3.6 years dominate in more than 30 percent area of the clusters and as well as for the whole country. Moreover, inter-annual cycles of 5–10 years also show a relatively higher percentage of the area across all the clusters. Another interesting point which could be observed from Fig. 13 is that the percentage of area under significant peaks have almost similar value for all the clusters which imply that the significant periodicities would spread uniformly across all the regions of India. Further in future, both the RCPs shows almost similar values of periodicity which suggests that the impact of climate change on the periodicity will be insignificant.

3.8. Discussion

Close scrutiny of the results presented above indicates that the CERFACS-CNRM-CM5-IITM-RegCM4 performs better than other individual models and that of the Ensemble average in simulating the past observed precipitation and temperature. Also, selected RCM model is found to capture the drought trends in various regions of India satisfactorily. For most of the clusters, the rate of increase of the potential evapotranspiration (PET) is expected to be higher than the rate of increase in precipitation. However, the magnitude of increase in precipitation is much higher than the evapotranspiration in clusters 2 and 6 and, therefore, the change in evapotranspiration does not affect the drought dynamics, which makes it inefficient for causing drought in these regions. Furthermore, trend analysis reveals that the historical increasing severity trend are concentrated over northcentral and southcentral regions of India which may continue to remain same in near future for RCP 4.5. However, a westward shift may be expected for higher GHG concentration. A decreasing trend in the severity and frequency under RCP 8.5 is likely in eastern states such as Odisha and Chhattisgarh in the far future. The results of analysis of annual maximum drought affected area reveals the dominance of the evapotranspiration in forming the droughts in Clusters 3, 4 and 5 which spreads over most parts of the country. Moreover, RCP 8.5 may cause more risk over most parts of India since the drought hazard projected

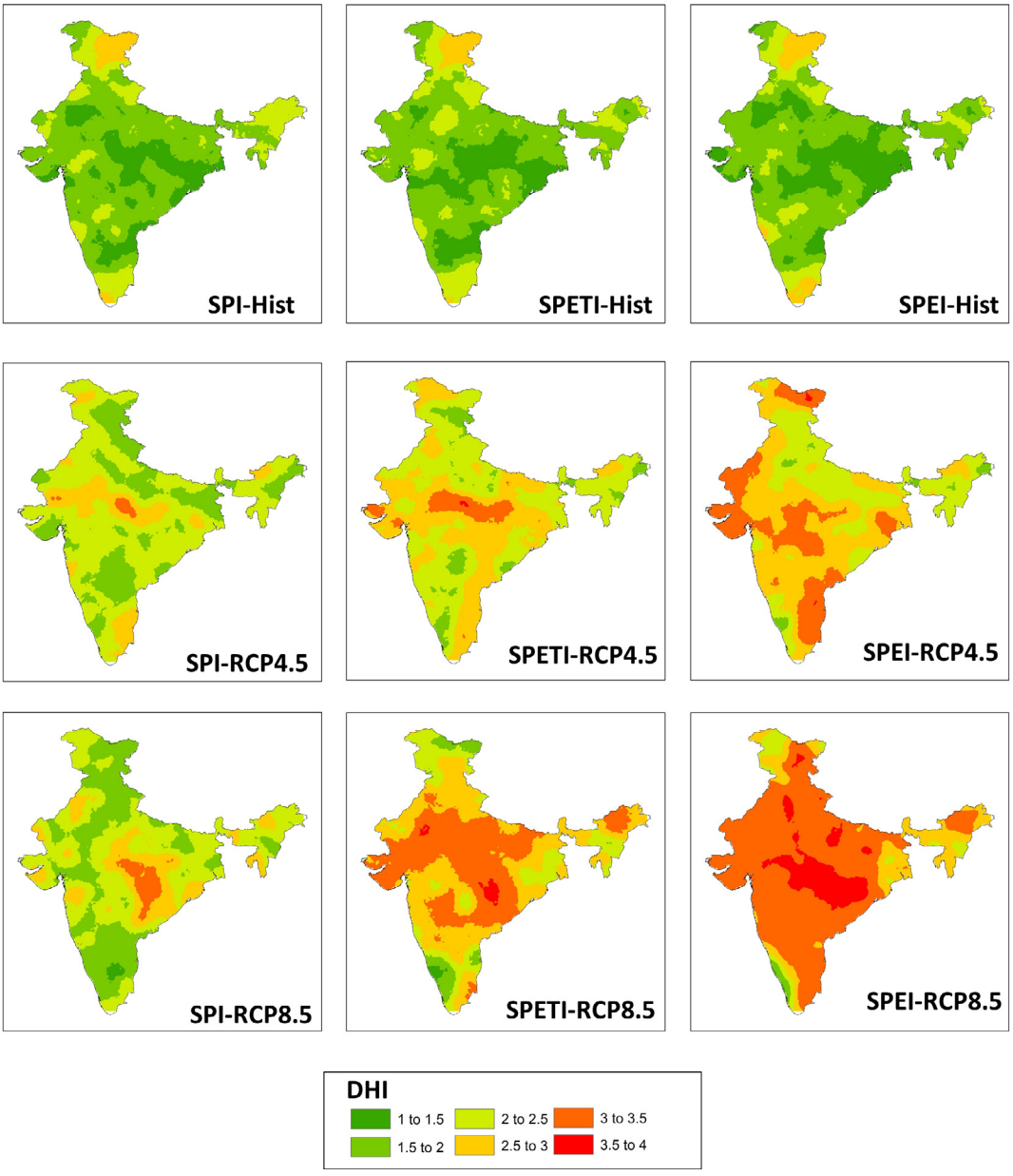

Fig. 12. Spatial Distribution of Drought Hazard Index (DHI) over India for Historical droughts (Hist) and future projected droughts under RCP 4.5 and RCP 8.5 for various drought indicators.

using this RCP is significantly higher than that of the RCP 4.5. Findings of drought periodicity analysis reveal the presence of dominant drought cycles of 2–3.6 years during the 1st half as well as the 2nd half of the 21st century indicating insignificant impact of climate change on drought periodicity.

Past studies suggest that droughts are having positive trends of intensity, frequency and severity owing to declining trends in precipitation (Mallya et al., 2016; Naresh Kumar et al., 2012; Jain and Kumar,

Table 6
Average values of Drought Hazard Index for different clusters.

		Cluster 1	Cluster 2	Cluster 3	Cluster 4	Cluster 5	Cluster 6	All India
Hist	SPI	2.671	2.044	1.750	1.581	1.807	2.059	1.798
	SPETI	2.619	2.022	1.693	1.571	1.886	1.921	1.786
	SPEI	2.608	2.096	1.818	1.499	1.746	1.824	1.740
RCP4.5	SPI	2.056	2.283	2.150	2.197	2.247	2.135	2.194
	SPETI	2.236	2.270	2.410	2.581	2.543	2.207	2.472
	SPEI	2.935	2.401	2.901	2.653	2.741	2.261	2.707
RCP8.5	SPI	1.880	2.007	1.980	2.488	2.134	2.297	2.199
	SPETI	2.458	1.941	2.655	2.987	2.909	2.651	2.801
	SPEI	3.088	2.125	3.241	3.302	3.256	2.788	3.181

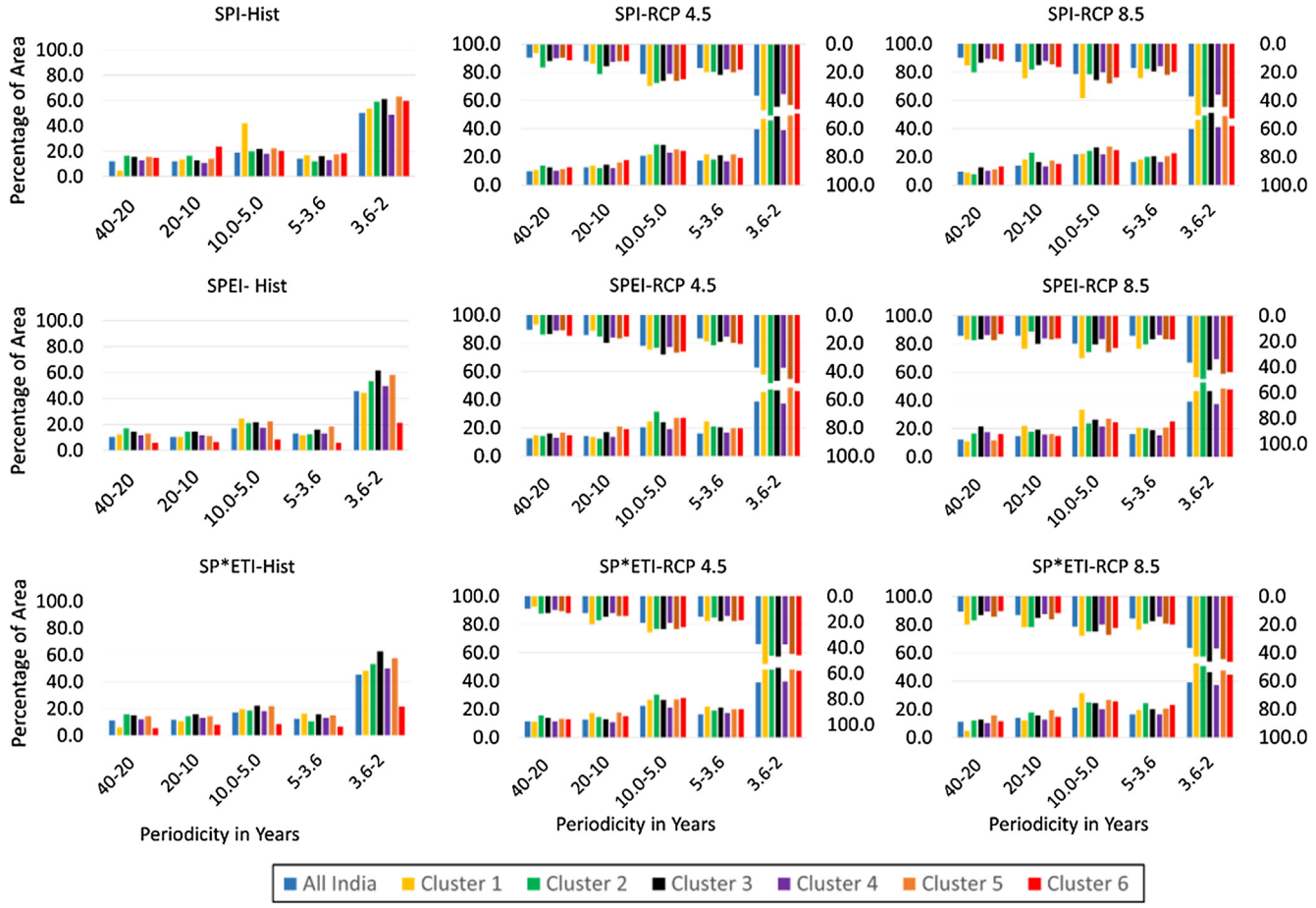

Fig. 13. Average percentage of area for monsoon months which shows significant peaks for different periodicities. Grouped bars on lower X-axis represents dominant average periodicities in first half of the century and corresponding percentage of area can be read on left Y-axis and grouped bars on upper X-axis represents dominant average periodicities in second half of the century and corresponding percentage of area can be read on right Y-axis.

2012) which also validates the findings of this study. However, studies based on analysis of future projected CMIP5 multi-model data suggest that the Indian Monsoon precipitation may increase in the 21st century due to the favourable relationship between warming and the amount of Indian summer monsoon (Turner and Annamalai, 2012). Also, it is expected that the increase in precipitation for RCP 8.5 would be greater than lower emission RCPs (Menon et al. 2013, Kundu et al., 2014; Chaturvedi et al., 2012; Freychet et al., 2015). This corroborates favourably with findings such as existence of positive correlation between the Indian summer monsoon for most of the clusters and global warming (Fu et al., 1999); increase in the seasonal precipitation due to changes in inter-tropical convergence zone (Hu et al., 2000) and warming of the sea surface combined with the amplified vapour holding capacity would lead to more water vapour content in the atmosphere resulting in enhanced precipitation in the tropics (Trenberth, 1998; Meehl et al., 2005). Alam et al. (2017) used the SPEI and found an increment in the probability of occurrence of drought in the six different ecological regions of India. Furthermore, Nath et al. (2017) found a consistent increase in the precipitation and evapotranspiration; however, the increase in PET for a higher emission scenario will be much higher than the projected increase in the precipitation for the 21st century. The mitigating effect of the increased precipitation on drought in RCP 4.5 will be overridden by the intensification in PET (Nath et al., 2017). It is important to notice that the drought intensification in the past over India was driven by the decreasing trend in precipitation. However, in the future, the drought intensification would be driven by the escalation of evapotranspiration. This study establishes a clear link between the alteration in precipitation and temperature and changes in the drought characteristics for different regions of India for various carbon emission scenarios. Findings of this study also underscore the need to choose drought index carefully for drought characterisation under the climate change scenario because the rise in temperature has different effects on precipitation as well as on evapotranspiration which may result in different drought scenarios. Special care should be exercised in interpreting the results obtained based on the SPEI when the rise in temperature of higher order have been predicted due to global warming as it may project extreme drought scenario due to the assumption of ET to take place at the potential rate. Therefore, drought indices which consider the realistic representation of increase in the ET should be preferred. The findings of our study are in conformity with the previous studies referred above because the projected increase in the amount of precipitation may lead to reduced drought risk; however, an increase in the evapotranspiration due to the projected increase in temperature is likely to surpass projected increase in precipitation over most parts of the country that may result in increased drought risk.

The periodicity analysis indicates inter-annual periodicities influencing monsoon months to be distributed uniformly across all clusters of the Indian subcontinent with an average cycle of 2–3.6 years dominating the country. Inter-annual periodicities of short and long durations (such as 2–4 years and 4–8 years) may be correlated with Quasi-Biennial Oscillation (QBO) and El Niño–Southern Oscillation (ENSO) phenomenon (Adarsh and Janga Reddy, 2015; Kumar et al., 2013; Gadgil et al., 2007) because QBO and ENSO affects the Indian Summer Monsoon Rainfall (Kumar et al., 2013). However, long term inter-decadal periodicities may be correlated to Pacific Decadal Oscillation

(PDO) and Atlantic Multidecadal Oscillation (Joshi and Kucharski, 2017). Kripalani et al. (2003) found ENSO phenomenon to be negatively correlated with Indian summer monsoon rainfall. Moreover, Kumar et al. (2013) suggested that ENSO plays an important role in causing monsoon drought in the Indian region.

Results of this study may have serious implications on the policy making and water resource planning and management of India. The results suggest an increment in drought affected area, especially in Clusters 3, 4 and 5, where the population is much higher than in the other clusters. According to the UN population projection (2017), the total population of India may increase up to 1.8 billion by the year 2050 and to 2 billion by the year 2100. Increase in the population will increase the stress on the resources of water and food. Further, as previously reported by Jülich (2011), drought trigger migration has been taking place from eastern villages of the country to the south Indian cities. The drought triggered migration may intensify in future. The agricultural GDP has reduced from 39% in 1983 to 14% in 2014 (GOI, 2016). Reduced agricultural area and increased population along with the severe droughts in the regions where most people live may pose serious risk to food security in India. Out of 33.23% of installed renewable power generation, hydropower contributes toward almost 13.17% of total installed capacity. Hydropower plants installed in Clusters 3 and 4, alone contributes around 32% of total hydropower. Reduction in the water availability in reservoirs due to longer and severe droughts in these regions may drastically reduce the amount of hydropower generation. Therefore, enhanced preparedness is needed in the light of these results to alleviate the drought risk in these regions in the future. Policies should be framed while considering regional vulnerabilities and projected hazard.

Further, it is important to mention various uncertainties which are inherent in almost all studies based on the projected future climatic scenarios and the same are also involved in the presented analysis as well. Uncertainty related to GCM simulation such as uncertainty in simulating large-scale atmospheric circulation, inter-GCM projection uncertainty, emission scenario uncertainty and downscaling model uncertainty may lead to lesser confidence in the obtained drought results. Spatial resolution and choice of drought indices and its scale may also affect the drought projections. However, in the future, a better understanding of hydrological cycle may lead to better and less uncertain projections thus leading to better future climatic predictions that may reduce uncertainty in drought analysis.

4. Conclusions

Spatiotemporal analysis of likely occurrence and distribution of droughts was performed over India using 81 years (2021–2100) of projected precipitation and temperature data obtained from CERFACS-CNRM-CM5-IITM-RegCM4 RCM for two RCP scenarios (RCP 4.5 and RCP 8.5), and historical observed data (1951–2005) obtained from the IMD in gridded form, respectively. Temporal trends of drought severity and frequency were also analyzed. Drought hazard maps were prepared using the drought hazard index (DHI). Periodicity analysis was also carried out using Fourier transform to find the hidden periodicities in SPI, SP*ETI and SPEI series of monsoon months.

Results of regionalization in India suggest the presence of 6 distinct homogeneous drought regions in India. Precipitation, temperature and PET are found to be increasing in the 21st century for almost all the clusters. Analysis of projected scenarios of drought based on multiple indices for 21st century reveals that global warming may have severe impact on the drought scenario in India. Analysis of results indicates that the SPI projects least drought risk in the far future due to increasing precipitation. A significant correlation between all studied drought indicators have been found for historical period. However, for future, ET based drought indices such as SP*ETI and SPEI shows a more intense drought, especially in the later part of the 21st century. Interestingly, comparison of results obtained using different drought indices for various climate change scenarios underscore the importance of considering rise in evapotranspiration due to increase in temperature in drought characterisation. Failure to do so may result in the introduction of uncertainty in the end results. However, special care should be exercised in interpreting results obtained based on SPEI when the rise in temperature of higher order have been projected due to global warming because it may predict extreme drought scenario due to the assumption of ET to take place at potential rate. Therefore, drought indices which consider the realistic representation of increase in ET should be preferred. Therefore, for drought characteristics investigation under the climate change, this study clearly recommends to use the multiple ET based drought indices to arrive at the final conclusion.

Results of trend analysis suggest that Northern and North-western India may face increasing trends in severity and frequency of drought in the near future (NF). However, in the far future (FF) most parts of the India are expected to face increasing severity and frequency of drought except south-eastern regions such as Odisha, Chhattisgarh and parts of Maharashtra, Madhya Pradesh and Telangana. These increasing trends relies solely on increase in ET values in these regions. Analysis of Drought Hazard Index (DHI) reveals a shift in drought hazard from central India towards southeast-central India with an increase in GHG concentration considering all the drought indices. Impact of increase in evapotranspiration would be more pronounced on the occurrence of drought in Cluster 3 (Southern India), Cluster 4 (Central and southeast region) and Cluster 5 (North-western and western India) because in these clusters, both the ET based drought indices show a larger areal extent under drought for these regions in the far future. Further, for these regions, average Drought Hazard Index has also been found to be larger than other regions. Interannual significant periodicities of 2–3.6 years are likely to be distributed uniformly across all clusters of drought regions of India during the 21st century. Moreover, change in drought periodicity due to climate change in most of the regions has been found to be insignificant.

Acknowledgements

This research did not receive any specific grant from funding agencies in the public, commercial, or not-for-profit sectors. However, authors are very thankful to Indian Institute of Technology Roorkee, India for providing the necessary resources to conduct this research and Ministry of Human Resources, Govt. of India for supporting first author through Senior Research Fellowship.

References

Adarsh, S., Janga Reddy, M., 2015. Trend analysis of rainfall in four meteorological subdivisions of southern India using nonparametric methods and discrete wavelet transforms. Int. J. Climatol. 35 (6), 1107–1124.
Alam, N.M., Sharma, G.C., Moreira, E., Jana, C., Mishra, P.K., Sharma, N.K., Mandal, D., 2017. Evaluation of drought using SPEI drought class transitions and log-linear models for different agro-ecological regions of India. Phys. Chem. Earth Parts A/B/C 100, 31–43.
Ashfaq, M., Shi, Y., Tung, W.W., Trapp, R.J., Gao, X., Pal, J.S., Diffenbaugh, N.S., 2009. Suppression of south Asian summer monsoon precipitation in the 21st century. Geophys. Res. Lett. 36 (1).
Bhalme, H.N., Mooley, D.A., 1980. Large-scale droughts/floods and monsoon circulation. Mon. Weather Rev. 108 (8), 1197–1211.
Bharati, S., Som, S., Bharati, P., Vasulu, T.S., 2001. Climate and head form in India. Am. J. Hum. Biol.: Off. J. Hum. Biol. Assoc. 13 (5), 626–634.
Bloomfield, P., 2004. Fourier Analysis of Time Series: An Introduction. John Wiley & Sons.
Bordi, I., Fraedrich, K., Gerstengarbe, F.W., Werner, P.C., Sutera, A., 2004. Potential predictability of dry and wet periods: Sicily and Elbe-Basin (Germany). Theor. Appl. Climatol. 77 (3–4), 125–138.
Burke, E.J., Brown, S.J., Christidis, N., 2006. Modeling the recent evolution of global drought and projections for the twenty-first century with the Hadley Centre climate model. J. Hydrometeorol. 7 (5), 1113–1125.
Burn, D.H., 1990. Evaluation of regional flood frequency analysis with a region of influence approach. Water Resour. Res. 26 (10), 2257–2265.
Byun, H.R., Wilhite, D.A., 1999. Objective quantification of drought severity and duration. J. Clim. 12 (9), 2747–2756.
Chaturvedi, R.K., Joshi, J., Jayaraman, M., Bala, G., Ravindranath, N.H., 2012. Multi-

model climate change projections for India under representative concentration pathways. Curr. Sci. 103 (7), 791–802.
Chowdhury, A., Dandekar, M.M., Raut, P.S., 1989. Variability in drought incidence over India–a statistical approach. Mausam 40 (2), 207–214.
Cook, E.R., Meko, D.M., Stahle, D.W., Cleaveland, M.K., 1999. Drought reconstructions for the continental United States. J. Clim. 12 (4), 1145–1162.
Cubasch, U., Meehl, G.A., Boer, G.J., Stouffer, R.J., Dix, M., Noda, A., … Yap, K.S., 2001. Projections of future climate change. In: Houghton, J,T., Ding, Y., Griggs, D.J., Noguer, M., Van der Linden, P.J., Dai, X., Maskell, K., Johnson, C.A. (Eds.), Climate Change 2001: The Scientific Basis: Contribution of Working Group I to the Third Assessment Report of the Intergovernmental Panel. pp. 526–582.
Dai, A., 2013. Increasing drought under global warming in observations and models. Nat. Clim. Change 3 (1), 52–58.
Dalton, L., Ballarin, V., Brun, M., 2009. Clustering algorithms: on learning, validation, performance, and applications to genomics. Curr. Genomics 10 (6), 430–445.
Daneshvar, M.R.M., Bagherzadeh, A., Khosravi, M., 2013. Assessment of drought hazard impact on wheat cultivation using standardized precipitation index in Iran. Arabian J. Geosci. 6 (11), 4463–4473.
Das, P.K., Dutta, D., Sharma, J.R., Dadhwal, V.K., 2016. Trends and behaviour of meteorological drought (1901–2008) over Indian region using standardized precipitation–evapotranspiration index. Int. J. Climatol. 36 (2), 909–916.
Davies, D.L., Bouldin, D.W., 1979. A cluster separation measure. IEEE Trans. Pattern Anal. Mach. Intell. 2, 224–227.
Dogan, S., Berktay, A., Singh, V.P., 2012. Comparison of multi-monthly rainfall-based drought severity indices, with application to semi-arid Konya closed basin, Turkey. J. Hydrol. 470, 255–268.
Dunn, J.C., 1974. Well-separated clusters and optimal fuzzy partitions. J. Zybernetics 4 (1), 95–104.
Fan, K., Liu, Y., Chen, H., 2012. Improving the prediction of the East Asian summer monsoon: new approaches. Weather Forecasting 27 (4), 1017–1030.
Farahmand, A., AghaKouchak, A., 2015. A generalized framework for deriving nonparametric standardized drought indicators. Adv. Water Resour. 76, 140–145.
Freychet, N., Hsu, H.H., Chou, C., Wu, C.H., 2015. Asian summer monsoon in CMIP5 projections: a link between the change in extreme precipitation and monsoon dynamics. J. Clim. 28 (4), 1477–1493.
Fu, C., Diaz, H.F., Dong, D., Fletcher, J.O., 1999. Changes in atmospheric circulation over Northern Hemisphere oceans associated with the rapid warming of the 1920s. Int. J. Climatol. 19 (6), 581–606.
Gadgil, S., Rajeevan, M., Francis, P.A., 2007. Monsoon variability: Links to major oscillations over the equatorial Pacific and Indian oceans. Curr. Sci. 93 (2), 182–194.
Gibbs, W.J., Maher J.V., 1967. Rainfall deciles as drought indicators. Bureau of Meteorology Bull. 48, Commonwealth of Australia, Melbourne, Australia.
Gocic, M., Trajkovic, S., 2013. Analysis of changes in meteorological variables using Mann-Kendall and Sen's slope estimator statistical tests in Serbia. Global Planet. Change 100, 172–182.
GOI, 2016. State of Indian Agriculture 2015–16. Government of India, Ministry of Agriculture & Farmers Welfare, Department of Agriculture, Cooperation & Farmers Welfare, Directorate of Economics and Statistics, New Delhi.
Goyal, M.K., Gupta, V., 2014. Identification of homogeneous rainfall regimes in Northeast Region of India using fuzzy cluster analysis. Water Resour. Manage. 28 (13), 4491–4511.
Goyal, M.K., Gupta, V., Eslamian, S., 2017. Hydrological Drought: Water Surface and Duration Curve Indices. *Handbook of Drought and Water Scarcity: Principles of Drought and Water Scarcity*.
Guhathakurta, P., Rajeevan, M., 2008. Trends in the rainfall pattern over India. Int. J. Climatol. 28 (11), 1453–1470.
Gupta, A.K., Tyagi, P., Sehgal, V.K., 2011. Drought disaster challenges and mitigation in India: strategic appraisal. Curr. Sci. 1795–1806.
Hosking, J.R.M., Wallis, J.R., 1993. Some statistics useful in regional frequency analysis. Water Resour. Res. 29 (2), 271–281.
Hu, Z.Z., Latif, M., Roeckner, E., Bengtsson, L., 2000. Intensified Asian summer monsoon and its variability in a coupled model forced by increasing greenhouse gas concentrations. Geophys. Res. Lett. 27 (17), 2681.
Jain, S.K., Kumar, V., 2012. Trend analysis of rainfall and temperature data for India. Curr. Sci. 37–49.
Jain, V.K., Pandey, R.P., Jain, M.K., Byun, H.R., 2015. Comparison of drought indices for appraisal of drought characteristics in the Ken River Basin. Weather Clim. Extremes 8, 1–11.
Janga Reddy, M., Ganguli, P., 2012. Application of copulas for derivation of drought severity–duration–frequency curves. Hydrol. Process. 26 (11), 1672–1685.
Jha, S., Sehgal, V.K., Raghava, R., Sinha, M., 2013. Trend of standardized precipitation index during Indian summer monsoon season in agroclimatic zones of India. Earth Syst. Dyn. Discuss. 4 (1), 429–449.
Joetzjer, E., Douville, H., Delire, C., Ciais, P., Decharme, B., Tyteca, S., 2013. Hydrologic benchmarking of meteorological drought indices at interannual to climate change timescales: a case study over the Amazon and Mississippi river basins. Hydrol. Earth Syst. Sci. 17 (12), 4885.
Joshi, M.K., Kucharski, F., 2017. Impact of Interdecadal Pacific Oscillation on Indian summer monsoon rainfall: an assessment from CMIP5 climate models. Clim. Dyn. 48 (7–8), 2375–2391.
Jülich, S., 2011. Drought triggered temporary migration in an East Indian village. Int. Migr. 49, e189–e199.
Knutti, R., Sedláček, J., 2013. Robustness and uncertainties in the new CMIP5 climate model projections. Nat. Clim. Change 3 (4), 369–373.
Kogan, F.N., 1995. Droughts of the late 1980s in the United States as derived from NOAA polar-orbiting satellite data. Bull. Am. Meteorol. Soc. 76 (5), 655–668.
Kripalani, R.H., Kulkarni, A., Sabade, S.S., Khandekar, M.L., 2003. Indian monsoon variability in a global warming scenario. Nat. Hazards 29 (2), 189–206.
Kumar, K.R., Kumar, K.K., Pant, G.B., 1994. Diurnal asymmetry of surface temperature trends over India. Geophys. Res. Lett. 21 (8), 677–680.
Kumar, P., Wiltshire, A., Mathison, C., Asharaf, S., Ahrens, B., Lucas-Picher, P., Jacob, D., 2013. Downscaled climate change projections with uncertainty assessment over India using a high resolution multi-model approach. Sci. Total Environ. 468, S18–S30.
Kundu, A., Dwivedi, S., Chandra, V., 2014. Precipitation trend analysis over eastern region of India using CMIP5 based climatic models. Int. Arch. Photogramm. Remote Sens. Spatial Inf. Sci. 40 (8), 1437.
Lal, M., Nozawa, T., Emori, S., Harasawa, H., Takahashi, K., Kimoto, M., Numaguti, A., 2001. Future climate change: implications for Indian summer monsoon and its variability. Curr. Sci. 81 (9), 1196–1207.
Lal, M., Singh, S.K., 2001. Global warming and monsoon climate. Mausam 52 (1), 245–262.
Lenderink, G., Buishand, A., Deursen, W.V., 2007. Estimates of future discharges of the river Rhine using two scenario methodologies: direct versus delta approach. Hydrol. Earth Syst. Sci. 11 (3), 1145–1159.
Lin, W.A.N.G., Wen, C.H.E.N., Wen, Z., Gang, H.U.A.N.G., 2015. Drought in Southwest China: a review. Atmos. Oceanic Sci. Lett. 8 (6), 339–344.
Livada, I., Assimakopoulos, V.D., 2007. Spatial and temporal analysis of drought in Greece using the standardized precipitation index (SPI). Theor. Appl. Climatol. 89 (3–4), 143–153.
Lloyd-Hughes, B., 2012. A spatio-temporal structure-based approach to drought characterisation. Int. J. Climatol. 32 (3), 406–418.
Maccioni, P., Kossida, M., Brocca, L., Moramarco, T., 2014. Assessment of the drought hazard in the Tiber River Basin in Central Italy and a comparison of new and commonly used meteorological indicators. J. Hydrol. Eng. 20 (8), 05014029.
MacQueen, J., 1967. Some methods for classification and analysis of multivariate observations. In: Proceedings of the fifth Berkeley symposium on mathematical statistics and probability. vol. 1(14), pp. 281–297).
Maidment, D.R., 1992. Handbook of Hydrology. McGraw-Hill Inc.
Mallya, G., Mishra, V., Niyogi, D., Tripathi, S., Govindaraju, R.S., 2016. Trends and variability of droughts over the Indian monsoon region. Weather Clim. Extremes 12, 43–68.
Masud, M.B., Khaliq, M.N., Wheater, H.S., 2017. Future changes to drought characteristics over the Canadian Prairie Provinces based on NARCCAP multi-RCM ensemble. Clim. Dyn. 48 (7–8), 2685–2705.
May, W., 2002. Simulated changes of the Indian summer monsoon under enhanced greenhouse gas conditions in a global time-slice experiment. Geophys. Res. Lett. 29 (7).
McKee, T.B., Doesken, N.J., Kleist, J., 1993. In: The Relationship of Drought Frequency and Duration to Time Scales. American Meteorological Society, Boston, MA, pp. 179–183.
McSweeney, C.F., Jones, R.G., Lee, R.W., Rowell, D.P., 2015. Selecting CMIP5 GCMs for downscaling over multiple regions. Clim. Dyn. 44 (11–12), 3237–3260.
Meehl, G.A., Washington, W.M., Collins, W.D., Arblaster, J.M., Hu, A., Buja, L.E., Teng, H., 2005. How much more global warming and sea level rise? Science 307 (5716), 1769–1772.
Menon, A., Levermann, A., Schewe, J., Lehmann, J., Frieler, K., 2013. Consistent increase in Indian monsoon rainfall and its variability across CMIP-5 models. Earth Syst. Dyn. 4 (2), 287–300.
Mishra, A.K., Singh, V.P., 2011. Drought modeling–a review. J. Hydrol. 403 (1), 157–175.
Mondal, A., Kundu, S., Mukhopadhyay, A., 2012. Rainfall trend analysis by Mann-Kendall test: a case study of north-eastern part of Cuttack district, Orissa. Int. J. Geol. Earth Environ. Sci 2 (1), 70–78.
Moreira, E.E., Martins, D.S., Pereira, L.S., 2015. Assessing drought cycles in SPI time series using a Fourier analysis. Nat. Hazards Earth Syst. Sci. 15 (3), 571–585.
Myung, I.J., 2003. Tutorial on maximum likelihood estimation. J. Math. Psychol. 47 (1), 90–100.
Naresh Kumar, M., Murthy, C.S., Sesha Sai, M.V.R., Roy, P.S., 2012. Spatiotemporal analysis of meteorological drought variability in the Indian region using standardized precipitation index. Meteorol. Appl. 19 (2), 256–264.
Nath, R., Cui, X., Nath, D., Graf, H.F., Chen, W., Wang, L., Li, Q., 2017. CMIP5 multimodel projections of extreme weather events in the humid subtropical Gangetic Plain region of India. Earth's Future 5 (2), 224–239.
O'Brien, K., Leichenko, R., Kelkar, U., Venema, H., Aandahl, G., Tompkins, H., West, J., 2004. Mapping vulnerability to multiple stressors: climate change and globalization in India. Global Environ. Change 14 (4), 303–313.
Orlowsky, B., Seneviratne, S.I., 2013. Elusive drought: uncertainty in observed trends and short-and long-term CMIP5 projections. Hydrol. Earth Syst. Sci. 17 (5), 1765–1781.
Pai, D.S., Sridhar, L., Rajeevan, M., Sreejith, O.P., Satbhai, N.S., Mukhopadhyay, B., 2014. Development of a new high spatial resolution (0.25× 0.25) long period (1901–2010) daily gridded rainfall data set over India and its comparison with existing data sets over the region. Mausam 65 (1), 1–18.
Palmer, W.C., 1965. Meteorological Drought. US Department of Commerce, Weather Bureau, Washington, DC.
Parthasarathy, B., Rupa Kumar, K., Munot, A.A., 1996. Homogeneous Regional Summer Monsoon Rainfall over India: Interannual Variability and Teleconnections. Indian Institute of Tropical Meteorology Research Report No. RR-070. ISSN-0252-1075.
Pathak, P., Kalra, A., Ahmad, S., Bernardez, M., 2016. Wavelet-aided analysis to estimate seasonal variability and dominant periodicities in temperature, precipitation, and streamflow in the Midwestern United States. Water Resour. Manage. 1–17.
Pattanaik, D.R., 2007. Analysis of rainfall over different homogeneous regions of India in relation to variability in westward movement frequency of monsoon depressions. Nat. Hazards 40 (3), 635–646.

Pollock, D.S.G., Green, R.C., Nguyen, T. (Eds.), 1999. Handbook of Time Series Analysis, Signal Processing, and Dynamics. Academic Press.
Praveen, D., Ramachandran, A., Jaganathan, R., Krishnaveni, E., Palanivelu, K., 2016. Projecting Droughts in the Purview of Climate Change under RCP 4.5 for the Coastal Districts of South India. Indian J. Sci. Technol. 9 (6).
Rao, A.R., Srinivas, V.V., 2006a. Regionalization of watersheds by fuzzy cluster analysis. J. Hydrol. 318 (1), 57–79.
Rao, A.R., Srinivas, V.V., 2006b. Regionalization of watersheds by hybrid-cluster analysis. J. Hydrol. 318 (1), 37–56.
Rathore, B.M.S., Sud, R., Saxena, V., Rathore, L.S., Singh, T., Rathore, V.G.S., Roy, M.M., 2014. Drought conditions and management strategies in India. In: Country Workshop Report, Regional Workshop for Asia-Pacific, UN-Water Initiative on Capacity Development to Support National Drought Management Policies. pp. 6–9.
Razavi, S., Vogel, R., 2018. Prewhitening of hydroclimatic time series? implications for inferred change and variability across time scales. J. Hydrol. 557, 109–115.
Ridolfi, E., Rianna, M., Trani, G., Alfonso, L., Di Baldassarre, G., Napolitano, F., Russo, F., 2016. A new methodology to define homogeneous regions through an entropy based clustering method. Adv. Water Resour. 96, 237–250.
Rousseeuw, P.J., 1987. Silhouettes: a graphical aid to the interpretation and validation of cluster analysis. J. Comput. Appl. Math. 20, 53–65.
Saaty, T.L., 1977. A scaling method for priorities in hierarchical structures. J. Math. Psychol. 15 (3), 234–281.
Saha, S., Chakraborty, D., Choudhury, B.U., Singh, S.B., Chinza, N., Lalzarliana, C., Ngachan, S.V., 2015. Spatial variability in temporal trends of precipitation and its impact on the agricultural scenario of Mizoram. Curr. Sci. 109 (12), 2278–2282.
Salamalikis, V., Argiriou, A.A., Dotsika, E., 2016. Periodicity analysis of δ 18 O in precipitation over Central Europe: time–frequency considerations of the isotopic 'temperature' effect. J. Hydrol. 534, 150–163.
Sen Roy, S., Balling, R.C., 2004. Trends in extreme daily precipitation indices in India. Int. J. Climatol. 24 (4), 457–466.
Sengupta, A., Rajeevan, M., 2013. Uncertainty quantification and reliability analysis of CMIP5 projections for the Indian summer monsoon. Curr. Sci. 105 (12), 1692.
Shah, R., Bharadiya, N., Manekar, V., 2015. Drought index computation using standardized precipitation index (SPI) method for Surat district, Gujarat. Aquat. Proc. 4, 1243–1249.
Sheffield, J., Wood, E.F., Roderick, M.L., 2012. Little change in global drought over the past 60 years. Nature 491 (7424), 435–438.
Shivam, Goyal, M.K., Sarma, A.K., 2017. Analysis of the change in temperature trends in Subansiri River basin for RCP scenarios using CMIP5 datasets. Theor. Appl. Climatol. 129 (3–4), 1175–1187.
Singh, V., Sharma, A., Goyal, M.K., 2017. Projection of hydro-climatological changes over eastern Himalayan catchment by the evaluation of RegCM4 RCM and CMIP5 GCM models. Hydrol. Res nh2017193.
Sperber, K.R., Annamalai, H., Kang, I.S., Kitoh, A., Moise, A., Turner, A., Zhou, T., 2013. The Asian summer monsoon: an inter-comparison of CMIP5 vs. CMIP3 simulations of the late 20th century. Clim. Dyn. 41 (9–10), 2711–2744.
Strzepek, K., Yohe, G., Neumann, J., Boehlert, B., 2010. Characterizing changes in drought risk for the United States from climate change. Environ. Res. Lett. 5 (4), 044012.
Swain, S., Hayhoe, K., 2015. CMIP5 projected changes in spring and summer drought and wet conditions over North America. Clim. Dyn. 44 (9–10), 2737–2750.
Tabari, H., Somee, B.S., Zadeh, M.R., 2011. Testing for long-term trends in climatic variables in Iran. Atmos. Res. 100 (1), 132–140.
Tanaka, H.L., Ishizaki, N., Nohara, D., 2005. Intercomparison of the intensities and trends of Hadley, Walker and monsoon circulations in the global warming projections. SOLA 1, 77–80.
Telesca, L., Vicente-Serrano, S.M., López-Moreno, J.I., 2013. Power spectral characteristics of drought indices in the Ebro river basin at different temporal scales. Stoch. Env. Res. Risk Assess. 27 (5), 1155–1170.
Thilakarathne, M., Sridhar, V., 2017. Characterization of future drought conditions in the Lower Mekong River Basin. Weather Clim. Extremes 17, 47–58.
Thornthwaite, C.W., 1948. An approach toward a rational classification of climate. Geogr. Rev. 38 (1), 55–94.
Trenberth, K.E., 1998. Atmospheric moisture residence times and cycling: Implications for rainfall rates and climate change. Clim. Change 39 (4), 667–694.
Turner, A.G., Annamalai, H., 2012. Climate change and the South Asian summer monsoon. Nat. Clim. Change 2 (8), 587–595.
Ueda, H., Iwai, A., Kuwako, K., Hori, M.E., 2006. Impact of anthropogenic forcing on the Asian summer monsoon as simulated by eight GCMs. Geophys. Res. Lett. 33 (6).
UN, 2008. Trends in Sustainable Development 2008–2009. United Nations publication, United Nations Division for Sustainable Development.
UN Population projection, 2017. World Population Prospects: The 2017 Revision. Retrieved from: https://www.un.org/development/desa/publications/world-population-prospects-the-2017-revision.html On 01/08/2018.
Urcid, G., Ritter, G.X., 2012. Advances in Knowledge-Based and Intelligent Information and Engineering Systems. In: Graña, Manuel, Toro, Carlos, Posada, Jorge, Howlett, Robert J., Jain, Lakhmi C. (Eds.), Advances in Knowledge-Based and Intelligent Information and Engineering Systems. IOS Press, pp. 2140–2149.
USDA, 1970. 'Irrigation Water requirement' Tech. release N 21. USDA Soil Conservation Service, Washington, DC.
Vicente-Serrano, S.M., 2006. Differences in spatial patterns of drought on different time scales: an analysis of the Iberian Peninsula. Water Resour. Manage. 20 (1), 37–60.
Vicente-Serrano, S.M., Beguerıa, S., Lopez-Moreno, J.I., 2010. A multi-scalar drought index sensitive to global warming: the standardized precipitation evapotranspiration index—SPEI. J. Clim. 23, 1696–1718.
Von Storch, H., 1999. Misuses of statistical analysis in climate research. In: Analysis of Climate Variability. Springer, Berlin, Heidelberg, pp. 11–26.
Wang, L., Chen, W., 2014. A CMIP5 multimodel projection of future temperature, precipitation, and climatological drought in China. Int. J. Climatol. 34 (6), 2059–2078.
Wang, G., Wang, D., Trenberth, K.E., Erfanian, A., Yu, M., Bosilovich, M.G., Parr, D.T., 2017. The peak structure and future changes of the relationships between extreme precipitation and temperature. Nat. Clim. Change 7 (4), 268–274.
Wu, L.L., Zhang, W., Wu, T., 2013. Analysis of the periodicity of annual extreme runoff at Datong Station, Yangtze River, China. In: Applied Mechanics and Materials. Trans Tech Publications, pp. 2606–2610.
Xu, K., Yang, D., Yang, H., Li, Z., Qin, Y., Shen, Y., 2015. Spatio-temporal variation of drought in China during 1961–2012: A climatic perspective. J. Hydrol. 526, 253–264.
Yadava, M.G., Ramesh, R., 2007. Significant longer-term periodicities in the proxy record of the Indian monsoon rainfall. New Astron. 12 (7), 544–555.
Yevjevich, V.M., 1967. An objective approach to definitions and investigations of continental hydrologic droughts. Hydrology papers. Colorado State University No 23.
Yuan, F., Berndtsson, R., Zhang, L., Uvo, C.B., Hao, Z., Wang, X., Yasuda, H., 2015. Hydro climatic trend and periodicity for the Source Region of the Yellow River. J. Hydrol. Eng. 20 (10), 05015003.
Yue, S., Wang, C., 2004. The Mann-Kendall test modified by effective sample size to detect trend in serially correlated hydrological series. Water Resour. Manage. 18 (3), 201–218.
Zhang, Q., Singh, V.P., Li, K., Li, J., 2014. Trend, periodicity and abrupt change in streamflow of the East River, the Pearl River basin. Hydrol. Process. 28 (2), 305–314.